Physics – Uspekhi **53** (7) 725 – 745 (2010)

CONFERENCES AND SYMPOSIA

PACS numbers: 01.10.Fv, **75.47. – m**, **75.76. + j**, **76.30. – v**, **78.56. – a**, **85.75. – d**

Spintronics
(Scientific session of the Physical Sciences Division of the Russian Academy of Sciences, 3 February 2010)

DOI: 10.3367/UFNe.0180.201007g.0759

A scientific session of the Physical Sciences Division of the Russian Academy of Sciences (RAS) was held on 3 February 2010 at the Conference Hall of the P N Lebedev Physical Institute, RAS.

The following reports were put on the session agenda posted on the website www.gpad.ac.ru of the Physical Sciences Division, RAS:

(1) **Ustinov V V** (Institute of Metal Physics, Ural Branch, RAS, Ekaterinburg) "Metallic nanospintronics";

(2) **Kusrayev Yu G** (Ioffe Physical-Technical Institute, RAS, St. Petersburg) "Spin-related phenomena in semiconductors: physics and applications";

(3) **Tarasenko S A** (Ioffe Physical-Technical Institute, RAS, St. Petersburg) "Spin photocurrents in semiconductors";

(4) **Averkiev N S, Golub L E** (Ioffe Physical-Technical Institute, RAS, St. Petersburg) "Spin relaxation in quantum semiconductor heterostructures".

Papers written on the basis of reports 2–4 are given below.

Uspekhi Fizicheskikh Nauk **180** (7) 759 – 780 (2010)
DOI: 10.3367/UFNr.0180.201007g.0759
Translated by S N Gorin; edited by A Radzig

PACS numbers: **75.47. – m**, **75.76. + j**, **85.75. – d**
DOI: 10.3367/UFNe.0180.201007h.0759

Spin phenomena in semiconductors: physics and applications

Yu G Kusrayev

1. Introduction

Spin phenomena have been attracting progressively greater attention since the advent of the spin hypothesis advanced in 1925 by the Dutch physicists Samuel A Goudsmit and George E Uhlenbeck. The concept of spin rapidly won common recognition, since it solved the difficulties existing in spectroscopy at that time — those concerning explanations of the Zeeman effect and fine structure of spectral lines. The most informative method of investigation of spin phenomena in atoms and semiconductors appears to be the optical orientation of spins. The optical orientation of spins in atoms is assumed to have been discovered in 1924, when Wilhelm Hanle [1] correctly explained the famous experiments of Robert Wood [2] concerning the effect of a magnetic field on the polarized luminescence of the vapors of some metals. The general principles of this phenomenon were established in the early 1950s by the French group of Alfred Kastler [3]. He won the Nobel Prize in physics in 1966 "for the discovery and development of optical methods for studying Hertzian resonances in atoms." In 1968, Georges Lampel demonstrated for the first time the possibility of the optical orientation of conduction electron spins in semiconductors (Si) and the observation of their orientation by the nuclear magnetic resonance (NMR) method. A year later, the optical orientation of conduction electrons was observed in the semiconducting GaSb material using the polarization of luminescence [5]. From this time on, intense studies of spin-dependent phenomena in semiconductors started; the results of these studies were published in a collective monograph [6].

Simultaneously with the discovery of the optical orientation of electron spins, the great fundamental and practical importance of investigations of the generation and detection of spins by electrical methods was recognized. In 1971, M I D'yakonov and V I Perel' predicted the spin Hall effect, i.e., the appearance of a spin flow in the direction perpendicular to the electric current [7]. Experimentally, the spin generation by electric current was for the first time demonstrated in work [8]. In 1976, A G Aronov and G E Pikus suggested an idea for the production of nonequilibrium spin polarization in a semiconductor upon the passage of a current through a ferromagnetic contact with a semiconductor [9] (spin injection). Experimentally, spin injection was realized in GaAs by Alvarado and Renaud [10].

In the mid-1990s, a new burst of investigations occurred in spin physics, which was generated by the idea of using spin degrees of freedom in devices for the storage and processing of information. The electron spin that exists as a superposition of ground states $-1/2$ and $+1/2$ is a quantum analog of a classical bit of information. Such a *quantum bit* (*qubit*) can be used in various devices of spin logics. There appeared the term 'quantum computer' — a device that processes information presented in the form of a set of qubits rather than bits. Physical carriers of qubits, apart from electron spins, can be, for instance, photons (longitudinal

Yu G Kusrayev Ioffe Physical-Technical Institute, Russian Academy of Sciences, St. Petersburg, Russian Federation
E-mail: kusrayev@orient.ioffe.ru

Uspekhi Fizicheskikh Nauk **180** (7) 759 – 773 (2010)
DOI: 10.3367/UFNr.0180.201007h.0759
Translated by S N Gorin; edited by A Radzig

and transverse polarization) and nuclear spins. In 1990, a spin transistor was suggested [11]. The most impressive success in the field of spin electronics (*spintronics*) is the creation (on the basis of the giant magnetoresistance effect) of metallic spintronic devices (heads for reading hard disks, magnetic random access memory (MRAM), and others). For the discovery of giant magnetoresistance, Albert Fert and Peter Grünberg were awarded the Nobel Prize in Physics 2007 [12]. The latest advances in the fields of the transport and optical orientation of spins were described in a special issue of the journal *Semiconductor Science and Technology* [13], and in a recently published monograph [14].

2. Methods for studying spin phenomena in semiconductors

The most elegant and informative technique for the investigation of spin phenomena in semiconductors is the method of optical orientation of spins [6]. The absorption of circularly polarized light leads, in view of the law of preservation of the angular momentum, to the polarization of electron and hole spins (excitons). According to the selection rules for optical transitions, the recombination of spin-polarized charge carriers is accompanied by the emission of a circularly polarized radiation. The application of an external magnetic field causes spin precession and leads to a depolarization of the radiation — the so-called *Hanle effect*. The contour of magnetic depolarization $\rho(H)$ in the simplest case is described by a Lorentz contour with a half-width $\Delta H_{1/2} = \hbar/\mu g T_s$ and an amplitude $\rho_0 \propto T_s/\tau$, where $T_s = \tau\tau_s/(\tau + \tau_s)$, and τ and τ_s are the lifetime and spin-relaxation time, respectively.

The investigation of the polarization of radiation in a magnetic field makes it possible to reveal the fine details of the interaction of electrons with the surrounding medium and to determine the lifetime and the spin-relaxation time under stationary conditions (the precession period is a kind of time standard). Modern methods for the detection of weak optical fluxes make it possible to register the luminescence of single molecules and single quantum dots, and, consequently, the spin state of a *single* electron localized in a quantum dot. The direct method of studying spin dynamics also finds a successful application — the spectroscopy of time-resolved polarization of luminescence.

In recent years, a method based on the Faraday (or Kerr) effect has also found wide application, namely, a rotation of the plane of polarization of linearly polarized light upon its passage through a crystal (or reflection from a crystal) [14]. In this technique, two light sources (pulses) are used most frequently, one of which (circularly polarized) creates a nonequilibrium spin polarization, and the other (linearly polarized, with a variable time delay) dynamically registers this polarization with the use of the Faraday effect. In the English-language literature, this method is called the *pump-probe faraday rotation* (*PPFR*) *technique*. The sensitivity of the method of measuring the angle of polarization plane rotation is quite high, about 1 μrad, which makes it possible to determine the spin density to an accuracy of about ten Bohr magnetons per μm^3 (note for comparison that the magnetization of ferromagnets equal to $\sim 10^3$ G corresponds to 10^{11} spins/μm^3).

The electrical methods for the generation and detection of spins, especially in combination with optical methods, are applied quite efficiently to the investigation of spin transport, spin injection, and other phenomena (see Section 6, where the discoveries of the spin Hall effect and inverse spin Hall effect are discussed).

3. Optical orientation of spins in semiconductors

In cubic Ge and Si semiconductors (diamond structure) and in the majority of semiconducting III–V and II–VI compounds (zincblende structure), the conduction band of the s type near the edge of the forbidden band is twofold degenerate in spin ($s = \pm 1/2$), and the valence band of the p type is fourfold degenerate in the projection of the angular momentum J (heavy holes with $J = \pm 3/2$, and light holes with $J = \pm 1/2$). In accordance with the selection rules, the interband excitation by circularly polarized light leads to an orientation of the spins of electrons and holes. The spin-oriented charge carriers interact with phonons, impurities, and lattice nuclei, transferring their angular momenta to them. Because of the finite value of the lifetime, the charge carriers partially retain a nonequilibrium spin polarization. The phenomenon of optical spin orientation in semiconductors was first observed in silicon [4] by Lampel, who experimentally studied the effect of circularly polarized optical radiation on nuclear magnetic resonance. Figure 1 displays an NMR spectrum of ^{29}Si (pure silicon doped with phosphorus) prior to (curve *2*) and after (curve *1*) irradiation of the crystal by the circularly polarized light of a xenon lamp at the liquid-nitrogen temperature for 21 h. Curve *1* was obtained in a magnetic field of 1 G at $T = 77$ K, i.e., under conditions where the equilibrium nuclear polarization $P_{th} \propto H/T$ is negligible; curve *2* was recorded in a magnetic field of 6 kG at $T = 300$ K. The equilibrium nuclear polarization in the case of curve *1* is less by a factor of approximately 1500 and the NMR signal is several times greater than in the case of curve *2*, i.e., prior to the irradiation of the sample. The signal measured in a field of 1 G corresponds to the equilibrium polarization of nuclei in a

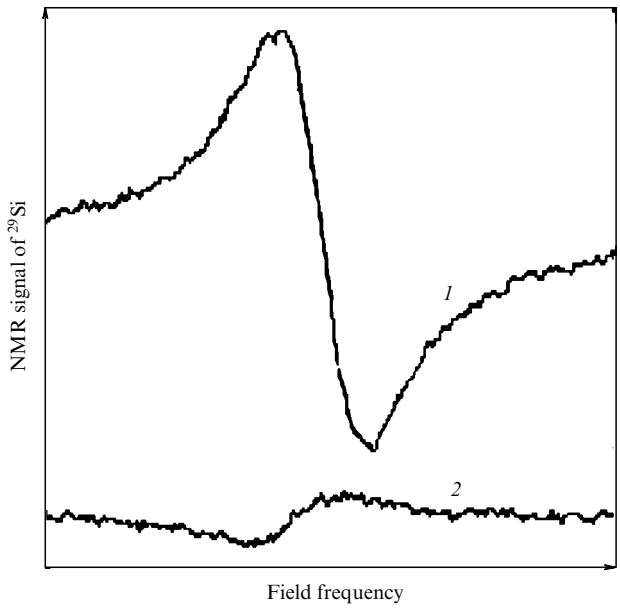

Figure 1. NMR signals of ^{29}Si [4]: *1* — signal obtained in a magnetic field $H = 1$ G after illumination of the sample by circularly polarized light at a temperature of 77 K for 21 h, and *2* — signal proportional to the equilibrium magnetization in a magnetic field $H = 6$ kG at a temperature of 300 K.

field of 15 kG ($T = 77$ K). In this experiment, two remarkable phenomena were observed simultaneously: optical orientation of electron spins by circularly polarized light, and a dynamic polarization of ^{29}Si nuclei caused by a hyperfine (contact) interaction with polarized electrons. The success of the experiment was mainly due to the large time of the spin–lattice relaxation of ^{29}Si nuclei equal to ≈ 200 h in the absence of illumination, and ≈ 20 h upon irradiation with interband light.

Later on, the optical spin orientation was observed in various semiconducting III–V, II–VI, and II–VII compounds [6]. The spin polarization of the charge carriers and excitons in these numerous experiments was registered based on the polarization of recombination radiation.

4. Spin interactions and spin relaxation

The variety of spin-related phenomena in semiconductors is determined by spin-dependent interactions. The main interactions here are (1) spin–orbit interaction, (2) hyperfine (contact) interaction, (3) electron–hole exchange interaction, and (4) exchange interaction of electrons with magnetic impurities.

The spin-orbit interaction plays the central role in spin phenomena and in spintronics:

(a) the optical spin orientation becomes possible due to the spin-orbit interaction, since the electric field of a light wave does not act directly on spins;

(b) most mechanisms of spin relaxation are connected with the spin–orbit interaction, since the perturbations in a crystal are mainly of electrical origin and do not act directly on spin, and, finally,

(c) the transport of charge carriers becomes spin-dependent because of the existence of spin–orbit coupling.

This also leads to the conclusion that is important for spintronics: spin–orbit interaction creates a unique possibility for the generation of spin polarization, control of spins, and detection (optical or electric) of spins.

Spin relaxation — disappearance of a nonequilibrium spin. Spin relaxation in most cases can be interpreted as a result of the action of effective (fluctuating in time) magnetic fields $\mathbf{H}_c$: the result of such an action depends on the frequency of precession in this field ($\omega \sim \mu g H_c/\hbar$) and a characteristic time (τ_c) of variation of this field, and is independent of the origin of fluctuating fields. The fluctuating fields are caused by various interactions including (a) spin–orbit (the Elliott–Yafet and D'yakonov–Perel' mechanisms), (b) electron–hole exchange (the Bir–Aronov–Pikus mechanism), (c) exchange interaction with a magnetic impurity, and (d) hyperfine (contact) interaction with nuclei.

The experimental investigation of dominating mechanisms of spin relaxation is an important and complex problem, since the rate of relaxation, on the one hand, determines the magnitude of the nonequilibrium spin and, on the other hand, depends on many factors, such as the spin interaction constants, temperature, concentration and type of an impurity, localization, and some others.

Let us briefly enumerate the main mechanisms of spin relaxation in semiconductors (for details, see Refs [6, 13, 14]).

(1) As a result of the mixing of states with an opposite spin orientation, spin flip becomes possible upon momentum scattering (the Elliott–Yafet mechanism) [15].

(2) Spin–orbit interaction in noncentrosymmetric semiconductors (GaAs is a typical representative) leads to band splitting in the case of nonzero wave vector $\mathbf{k}$ and is described by a Dresselhaus Hamiltonian [16]

$$\widehat{H}_{SO} = \hbar\boldsymbol{\sigma}\,\boldsymbol{\Omega}(\mathbf{k}),$$

$$\boldsymbol{\Omega}(\mathbf{k}) \propto \left[k_x(k_y^2 - k_z^2),\, k_y(k_z^2 - k_x^2),\, k_z(k_x^2 - k_y^2)\right]. \qquad (1)$$

The $\boldsymbol{\Omega}(\mathbf{k})$ vector can be interpreted as an effective $\mathbf{k}$-dependent magnetic field, and $\boldsymbol{\sigma} = (\sigma_x, \sigma_y, \sigma_z)$ are the Pauli matrices. The scattering of charge carriers leads to a random change in the magnitude and direction of $\boldsymbol{\Omega}(\mathbf{k})$ with characteristic time $\tau_c = \tau_p$ (where τ_p is the momentum relaxation time). The spin precession on the time interval between consecutive collisions leads to spin relaxation because of the uncorrelated nature of these acts. This mechanism was suggested by D'yakonov and Perel' [17]. In the approximation of small correlation times, when the angle of precession over the time interval between collisions is small ($\phi = \Omega\tau_p \ll 1$), the spin relaxation time can be estimated from the condition of the equality to unity of the root-mean-square deviation of spin from the initial direction: $(\Omega\tau_p)^2(\tau_s/\tau_p) \sim 1$, from which it follows that $\tau_s^{-1} \sim \Omega^2\tau_p$.

(3) The two other mechanisms are due to the exchange interaction. Spin flip occurs upon the exchange interaction of an electron with a hole (the Bir–Aronov–Pikus mechanism) [18]) or upon the interaction of a free electron with an electron bound at a paramagnetic center. The first scenario is realized in p-type semiconductors, while the second in dilute magnetic semiconductors. The Hamiltonian of the electron–hole exchange interaction is written out as $\widehat{H}_{exch} = A\mathbf{J}\,\mathbf{S}|\psi(r)|^2$, where A is the exchange constant, and $\mathbf{J}$ and $\mathbf{S}$ are the operators of the angular momentum of a hole (paramagnetic center) and electron spin, respectively. The spin relaxation can be considered as a precession in an effective magnetic field $\mathbf{H}_{eff} = A\mathbf{J}|\psi(\mathbf{r})|^2/\mu_B g$ (where g is the g factor of an electron), which fluctuates due to hole spin flips. In other words, the variable magnetic field $H_{eff}(t)$ causes transitions between electron spin sublevels. According to paper [19], the spin relaxation time in p-GaAs semiconductors with a concentration of acceptors $N_h = 4 \times 10^{18}$ cm^{-3} at low temperatures ($T < 100$ K) is determined by the exchange interaction with holes and is approximately 10^{-10} s.

The paramagnetic impurities also substantially decrease the spin relaxation time of charge carriers because of the presence of exchange interaction. The exchange field of magnetic impurities that acts on an electron can fluctuate because of either electron motion or spin–lattice relaxation of impurities. The experimental investigations show that in dilute magnetic semiconductors and in quantum wells (QWs) the time of spin relaxation of charge carriers does not exceed 10 ps [20–22]; the theory confirms the high efficiency of spin transfer from charge carriers to paramagnetic impurities [22, 23]. The exchange by spins occurs via a flip–flop mechanism in which the spins of a charge carrier and of a paramagnetic impurity flip into opposite directions and the total spin of the system is retained.

(4) The electron and nuclear spins in semiconductors are coupled by a contact Fermi interaction [24]:

$$\widehat{H}_{hf} = \sum_n a_n \mathbf{S}\mathbf{I}_n = \sum_n a_n \left(S_z I_n^z + \frac{S_+ I_n^- + S_- I_n^+}{2} \right), \qquad (2)$$

where $\mathbf{S}$ and $\mathbf{I}_n$ are the spins of an electron and of a nucleus located at a site n, $a_n = v_0 A|\Psi(\mathbf{r}_n)|^2$, v_0 is the volume of the unit cell, A is the hyperfine-interaction constant, $\Psi(\mathbf{r}_n)$ is the

envelope wave function of an electron, and $\mathbf{r}_n$ is the coordinate of the nucleus at the site n. In terms of the effective field, the contact Fermi interaction is equivalent to the action of a field $\mathbf{H}_{\rm eff} = \sum_n a_n \mathbf{I}_n/\mu_{\rm B} g$ from the surrounding nuclei on the electron. In a zero magnetic field, the electron spin $\mathbf{S}$ precesses in the hyperfine field $H_{\rm f} \approx H_{\max}/\sqrt{N}$ generated by the root-mean-square fluctuation of nuclear spins ($H_{\max}$ is the effective field of completely polarized nuclei, and N is the total number of nuclei in the interaction region). The field $H_{\rm f}$ has a random direction and its components perpendicular to S_z lead to electron spin relaxation. For free electrons, this mechanism is ineffective because of small $H_{\rm f}$ and $\tau_{\rm c}$ (the relaxation rate $\tau_{\rm s}^{-1} \sim \langle \Omega_{\rm f}^2 \rangle \tau_{\rm c}$ is proportional to the correlation time $\tau_{\rm c}$ and to the hyperfine field squared $H_{\rm f}^2$) [25]. The fluctuation fields and the correlation times increase substantially upon localization at a donor or at a semiconductor quantum dot (QD), where the probability density $|\Psi(\mathbf{r}_n)|^2$ of an electron location at a nucleus is high and the electron interacts simultaneously with a large number of nuclear spins ($N \sim 10^4 - 10^5$ nuclei). Typical values of the fields are as follows: $H_{\max} \sim 1$ T, and $H_{\rm f} \approx 10^{-2}$ T. The results of calculations show that the corresponding time of spin relaxation depends on the size of a QD (the Bohr radius of an electron at a donor) and in typical III–V and II–VI semiconductors ranges 1–10 ns [26].

It should be noted that the spin relaxation time of holes in crystals such as GaAs is significantly less than that of electrons. This is caused by the strong spin–orbit interaction in the valence band, which leads to a rigid coupling between the angular momentum and the hole momentum. Each event of scattering in this case leads to a loss of spin. The deformation or size quantization gives rise to a splitting of the band of heavy and light holes; as a result, the spin relaxation slows down. On the other hand, the symmetry of the hole wave function is such that the Bloch amplitude at the site of location of the nucleus becomes zero and, consequently, the contact interaction with the nuclei is absent.

Spin relaxation in n-GaAs. As an example of an experimental investigation of the electron spin relaxation in semiconductors, we shall consider the dependence of the spin relaxation time of electrons in n-GaAs on the concentration of donors $N_{\rm D}$ at low temperatures [27] (Fig. 2). One of the following mechanisms of electron spin relaxation usually dominates:

(a) hyperfine interaction with lattice nuclei at small donor concentrations $N_{\rm D} < 10^{15}$ cm^{-3}. The electron bound to a donor interacts with a large number of nuclei of the GaAs lattice, $N \sim 10^5$, and is affected by the fluctuation hyperfine field of lattice nuclei, $H_{\rm f} \propto 1/\sqrt{N}$. The magnitude of this field for a donor in GaAs is 54 Oe. As an electron jumps from donor to donor, the magnitude and the direction of the hyperfine field $\mathbf{H}_{\rm f}$ change, i.e., the correlation time $\tau_{\rm c}$ of the random field in this case is determined by the time of hopping. At frequent jumps from donor to donor, the spin relaxation time is given by the relation $\tau_{\rm s}^{-1} \sim \langle \Omega_{\rm f}^2 \rangle \tau_{\rm c}$;

(b) the D'yakonov–Perel' mechanism at a high concentration of donors, $N_{\rm D} > 2 \times 10^{16}$ cm^{-3}. The peculiarity at $N_{\rm D} = 2 \times 10^{16}$ cm^{-3} is due to the metal–insulator transition. This singularity reflects a change in the mechanism of spin relaxation. In the metallic phase, the electron scatters with a momentum transfer and suffers the action of a fluctuating spin–orbit field;

(c) at moderate concentrations of donors, $2 \times 10^{15} < N_{\rm D} < 2 \times 10^{16}$ cm^{-3} (the electron transfer between the donors occurs via tunneling), at which $\tau_{\rm s}$ decreases with increasing $N_{\rm D}$, the experimental results cannot be explained based on the above mechanisms; they yield overestimated times (low rate) of spin relaxation. In Ref. [28], K Kavokin suggested a new mechanism of spin relaxation for bound electrons in noncentrosymmetric systems. The exchange interaction between two donor electrons proves to be anisotropic and the mutual spin flip is accompanied by a precession of spins (in opposite directions) in the spin–orbit field by a certain angle $\pm\gamma$ dependent on the orientation of the donor pair. In an ensemble of donors with different γ, this process leads to a relaxation of the total spin of localized electrons. This mechanism gives a satisfactory explanation of experimental data. All three mechanisms considered above can be interpreted in terms of effective magnetic fields. As is seen from Fig. 2, at an optimum concentration of donors in n-GaAs the spin relaxation time at low temperatures exceeds 100 ns.

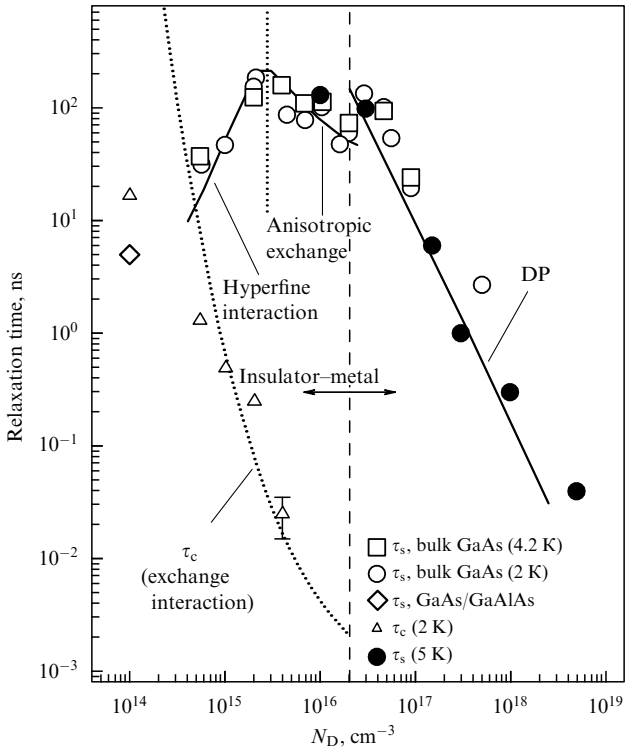

Figure 2. Time $\tau_{\rm s}$ of electron spin relaxation in gallium arsenide as a function of the donor concentration. The values of $\tau_{\rm s}$ were extracted from the results of experiments on the Hanle effect. The correlation times (triangles) were determined from the dependence of the circular polarization on the longitudinal magnetic field. DP: D'yakonov–Perel' mechanism (borrowed from Ref. [27]).

Spin relaxation in p-GaAs. As was noted above, the time of spin relaxation in p-GaAs at low temperatures ($T < 100$ K) is determined by the exchange interaction with holes and falls within the subnanosecond range. In GaAs doped with manganese, an unusual behavior of electron spin relaxation was revealed, which cannot be explained in terms of the above scheme for a p-type material. The impurity of Mn in GaAs serves simultaneously as an acceptor and a paramagnetic impurity. It could be expected that the spin relaxation caused by the exchange interaction of an electron with holes, on the one hand, and with paramagnetic centers, on the other hand, is quite efficient. However, as was shown experimentally [29], the spin relaxation time in GaAs:Mn

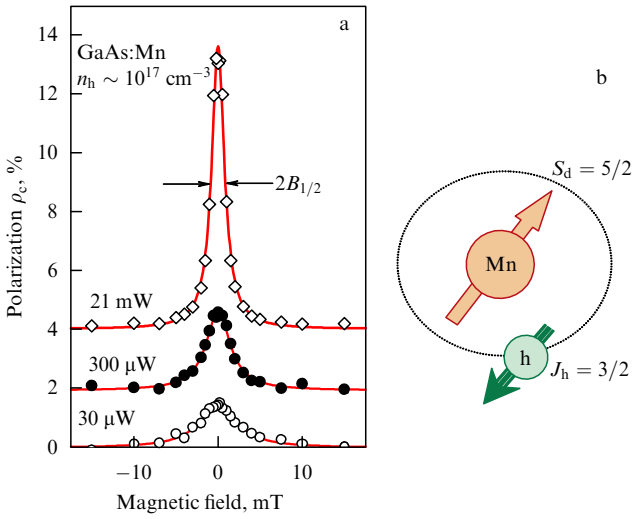

Figure 3. (a) Hanle effect in GaAs:Mn (p-GaAs) at various densities of optical excitation. The polarization of the photoluminescence is analyzed (donor–acceptor transition). The solid curves correspond to the approximation by a Lorentz contour. The spin relaxation time extracted from the experiment is about 100 ns; n_h is the concentration of holes. (b) Model of an Mn acceptor in GaAs: the hole in the Bohr orbit with a spin $J_h = 3/2$ (triple arrow) is involved in the exchange interaction with electrons localized in the d shell of manganese, $S_d = 5/2$ (arrow marked 'Mn'): $\widehat{H}_{pd}^{A^0} = -\Delta_{pd}\mathbf{S}_d\mathbf{J}_h$. In the ground state, the spins of manganese and the hole are oriented antiferromagnetically (borrowed from Ref. [29]).

proved to be very large. This is a unique situation, since two independent mechanisms of spin relaxation compensate for, rather than intensify, one another. Figure 3 displays curves of magnetic depolarization of radiation (the Hanle effect) in GaAs:Mn at various densities of optical excitation. The curves are well approximated by a Lorentz contour: the half-width of the contour and the degree of polarization made it possible to determine the spin relaxation time $\tau_s = 160$ ns for the maximum excitation density. The slowing down of electron spin relaxation found in p-GaAs occurs because of the compensation of the exchange interaction upon doping with magnetic impurities. Indeed, an electron interacts simultaneously with a hole localized at an acceptor and with electrons localized in the d shell of manganese (total spin $S_d = 5/2$). The interaction $\widehat{H}_{pd}^{A^0} = -\Delta_{pd}\mathbf{S}_d\mathbf{J}_h$ (the minus sign indicates the antiferromagnetic character of the interaction; the pd subscript corresponds to the p state of the valence band, and the d state of the magnetic impurity; the A^0 superscript corresponds to a neutral acceptor) splits the acceptor level into four sublevels which are characterized by the angular momentum $F = |S_d + J_h| = 1, 2, 3, 4$ [30]. In the ground state ($F = 1$), the spins of the Mn atom and the hole are oriented antiparallel, and the fluctuation fields generated by these spins compensate for each other almost completely [29]. In GaAs:Mn, a suppression of the spin relaxation of electrons was also observed in a longitudinal magnetic field. Using time-resolved luminescence spectroscopy, it was revealed that a weak magnetic field (2 kG) results in an increase in the spin relaxation time to $\tau_s = 1$ μs [31]. The effect of the magnetic field is related to the complete suppression of spin relaxation via the Bir–Aronov–Pikus mechanism.

Notice that the revealed slowing down of electron spin relaxation in p-type GaAs because of the mutual compensation of the exchange interaction upon doping with magnetic impurities opens new possibilities for constructing p–n junctions and magnetic memory devices. Since the state of a hole can be changed by deformation or by an applied electric field, an additional way for controlling spin degrees of freedom is coming into play.

Spin polarization of electrons at room temperature. A necessary condition for the operation of spintronic devices is a high electron spin polarization and its retention at *room temperature*. Unfortunately, the spin relaxation time in semiconductors at room temperature does not exceed several dozen picoseconds.

Thus, at present, an urgent problem is the search for and the investigation of materials with a large time of spin relaxation *at room temperature*. In papers [32–34], a new approach to the solution to this problem was developed. The idea reduces to the realization of such a situation where the spin dynamics of electrons is controlled by spin-dependent trapping by paramagnetic centers rather than by spin relaxation. It has been shown that this mechanism makes it possible to substantially increase the time of storage of spin polarization. The experiments on the optical orientation were carried out using $GaAs_{1-x}N_x$ solid solutions in which the nitrogen atoms stimulate the formation of complex defects with deep levels (an interstitial Ga atom surrounded by Group III or Group V atoms). It has been revealed that the optical spin polarization of free electrons is preserved at room temperature for more than 1 ns, which exceeds by an order of magnitude the theoretically predicted time of their spin relaxation. The degree of polarization in this case reaches 90%. It has been found that the anomalously large degrees of polarization and capacities of spin memory are due to the spin-dependent trapping of free electrons by deep paramagnetic centers, which leads to a dynamic polarization of the centers and the formation of a nonlinear coupled system of free and localized spins. The electrons localized at deep centers are less affected by the environment than the free electrons or electrons localized at shallow donors. Therefore, the deep paramagnetic centers retain their spin polarization for a longer time and, due to feedback, maintain the spin polarization of band electrons.

5. Spin processes in low-dimensional structures

The spin-related processes in low-dimensional structures have some features that distinguish them from processes in bulk crystals. Let us consider them in some detail.

Two-dimensional systems, quantum wells. The size quantization in the two-dimensional case fixes the component k_z of the wave vector in the direction of the axis of the QW (z-axis). For a structure grown from a noncentrosymmetric semiconductor this leads to the appearance of terms linear in the components k_x and k_y of the wave vector in the spin–orbit interaction. Indeed, by substituting the value of the size-quantized wave vector $k_z = \pi/\hbar L$ into the Dresselhaus Hamiltonian (1), we obtain in a linear approximation a Hamiltonian for a QW: $\widehat{H} = \beta(\sigma_x k_x - \sigma_y k_y)$. The value of the coefficient β depends on the width of the QW as $\beta \propto 1/L^2$, i.e., the narrower the QW, the greater the contribution of spin–orbit interaction.

The second feature of the QW is the presence of a contribution to the Hamiltonian that is caused by the asymmetry of the structure, i.e., by the absence of symmetry upon inversion of the axis of the QW. Such an asymmetry arises, for example, upon the application of an electric field along the z-axis or upon asymmetrical doping of the barriers

(if different concentrations of an impurity are introduced to the right and to the left of the QW). The corresponding contribution is described by the Rashba Hamiltonian $\hat{H}_{\rm R} = \alpha(\sigma_x k_y - \sigma_y k_x)$, in which the constant α depends on the degree of asymmetry of the QW [35]. Thus, a 'two-dimensional' electron is affected by an effective magnetic field that depends linearly on k and consists of two terms. The electron scattering leads to fluctuations of this field and, consequently, to spin relaxation. The theoretical problem of electron spin relaxation in a two-dimensional system was solved in Ref. [36]. An important advantage of two-dimensional systems is that, by changing the parameters of the QW, we can control the spectrum of electron states and the spin–orbit interaction. The specific features of spin relaxation in two-dimensional structures are described in detail in Ref. [37].

Let us briefly consider one very important effect, namely, the influence of an external electric field on the spin polarization of electrons. If we apply an electric field **E** to a sample, a directional motion of electrons with an average drift velocity $\mathbf{v}_{\rm d} \propto \mathbf{E}$ sets in. The electrons will feel the influence of a regular (rather than only fluctuational) effective magnetic field $\langle \mathbf{H}_{\rm eff} \rangle \propto \mathbf{v}_{\rm d}$. The action of such a regular field was revealed experimentally [38] when passing electric current along the plane of a GaAs/GaAlAs QW structure. A shift of the Hanle curve was observed, which was proportional to the electric current (Fig. 4). The shift was explained by the induction of an effective magnetic field due to spin–orbit interaction. In the presence of an electric current, the precession of the electron spin occurs in a field $\mathbf{H} = \mathbf{H}_0 + \langle \mathbf{H}_{\rm eff} \rangle$, which is determined by the sum of an external field $\mathbf{H}_0$ and spin–orbit field $\langle \mathbf{H}_{\rm eff} \rangle$; as a result, the Hanle curve $\rho(H)$ is shifted by $\langle \mathbf{H}_{\rm eff} \rangle$. An estimate for a GaAs/GaAlAs QW with a width $L = 10$ nm, an effective electron mass $m = 0.066 m_0$ (m_0 is the mass of a free electron), and a mobility $\mu \sim 10^4$ cm V^{-1} s^{-1} in an electric field $E = 10$ V cm^{-1} yields $\langle \mathbf{H}_{\rm eff} \rangle = 1.1 \times 10^{-2} \mu E$ cm^2 V^{-1} s ≈ 1 kOe. As is seen from Fig. 4, the shift of the Hanle curve is close to this estimate. This effect can be employed for a rapid and controlled change in spin using an electric current.

Optical orientation of spins in quantum dots. A most remarkable property of quantum dots (QDs), which makes them attractive for both fundamental investigations and numerous applications, is the discrete character of their energy structure. This discreteness of the energy spectrum leads to a strong suppression of the mechanisms of spin relaxation related to the spin–orbit interaction [39, 40]. Indeed, the absence of energy states between the levels of a QD should lead to more rigid (compared to those existing in bulk semiconductors or in QWs) selection rules upon spin transitions and to a slowing down of the spin relaxation rate. A long lifetime of a spin of an electron localized in a QD yields the fundamental possibility of using it for the realization of a quantum bit.

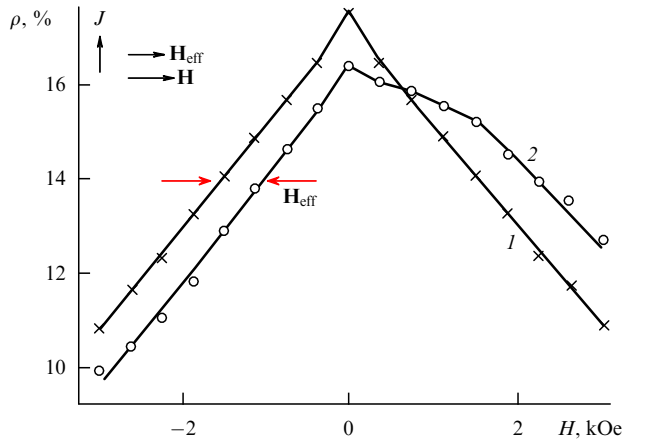

Figure 4. Hanle effect in a GaAs/GaAlAs QW. Curve *2* was obtained upon passing of electric current along the QW, and curve *1* was obtained in the absence of electric current (borrowed from Ref. [38]).

However, experiments on optical spin orientation in QDs under a continuous excitation revealed the absence of a circular polarization of radiation. The time-resolved measurements also showed a rapid decay of the signal of spin polarization of excitons [41]. It turned out that because of a strong electron–hole exchange interaction the exciton rapidly loses spin polarization. However, in a magnetic field parallel to the growth axis of the structure there appeared a noticeable signal of optical spin orientation; this effect is called the *restoration of optical orientation* [42]. When explaining experiments on the optical orientation of spins in QDs, it is necessary to take into account the anisotropic character of electron–hole exchange interaction (nanostructures, as a rule, exhibit a low symmetry, namely, C_{2v} or even lower). The anisotropic part of the exchange interaction leads to an additional splitting of exciton Zeeman sublevels. It has been shown theoretically [43, 44] and experimentally [45] that in nanostructures with a C_{2v} symmetry the radiation doublet of excitons with projections of the angular momentum $m_z = \pm 1$ (z is the growth axis of the structure) is split into two sublevels, $|X\rangle$ and $|Y\rangle$, that are dipole-active in two orthogonal linear polarizations of light. Linearly polarized light creates excitons with a given direction of the vector of the oscillating dipole moment, i.e., it gives rise to optical alignment [6]. Upon excitation by a pulse of circularly polarized radiation, a circular dipole in a superposition state $(|X\rangle + {\rm i}|Y\rangle)/\sqrt{2}$ is created. The evolution of this state in time is accompanied by oscillations of the circular polarization with a frequency $\omega = \omega_X - \omega_Y$ (these oscillations are frequently called quantum beats). In an ensemble of quantum dots, the signal decays rapidly because of the spread of precession frequencies (inhomogeneous broadening) [41, 46] and the oscillations can hardly be observed. For the same reason, the signal of optical orientation is also absent in the case of stationary excitation. If a longitudinal magnetic field is applied, the exciton states $|X\rangle$ and $|Y\rangle$ are transformed from linear dipoles in a zero or weak field ($H \ll \hbar\omega/\mu_{\rm B} g$) into circular dipoles in a strong field ($H \gg \hbar\omega/\mu_{\rm B} g$). In a strong magnetic field, a high circular polarization is observed, since it is determined by the long time of spin relaxation (the ratio $\tau_{\rm s}/(\tau + \tau_{\rm s})$ is close to unity). In intermediate magnetic fields, the exciton states represent a mixture of a linear and a circular dipole. If we excite an exciton in such a mixed state, the recombination radiation will be elliptically polarized. This leads to a new phenomenon—a conversion of the optical orientation into optical alignment and vice versa [47]. The conversion effect was examined experimentally in self-assembled QDs on the basis of semiconducting III–V [40] and II–VI [48, 49] compounds.

The situation is different in doped QDs: the optical excitation in this case leads to the formation of a singly charged exciton complex — a trion — which consists of two holes and one electron or two electrons and one hole (the charge of a QD can also be changed by applying an external

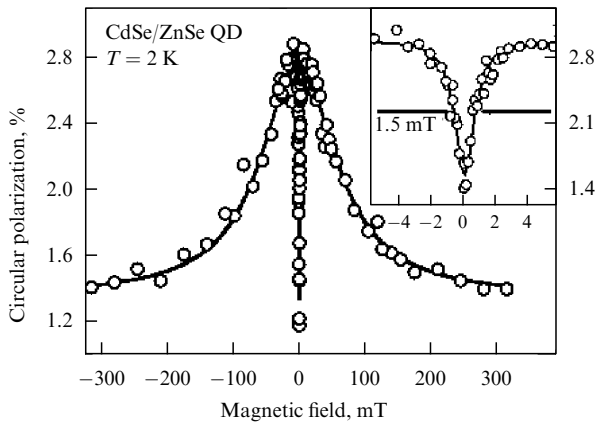

Figure 5. Degree of circular polarization as a function of the magnetic field induction (Hanle effect) in negatively charged CdSe/ZnSe QDs. The detection is performed on the line of the X^- trion. The solid curve represents a combined Lorentz contour $P_C(B) = P_e/[1 + (H/H^e_{1/2})^2] + P_h/[1 + (H/H^h_{1/2})^2]$ with half-widths $H^e_{1/2} = 0.75$ mT and $H^h_{1/2} = 70$ mT (borrowed from Ref. [54]).

electric field). In the ground state of the trion, two identical charge carriers form a spin singlet ($S_h = 0$ or $S_e = 0$), and the exchange interaction disappears [50, 51]. In charged dots, the optical spin orientation of both nonequilibrium and equilibrium (resident) charge carriers can be observed [52] (an analog of optical orientation in the ground state of atoms [3]). Using the direct method of time-resolved spectroscopy, the time of spin relaxation of holes in InAs/GaAs QDs was measured to be $\tau_{sh} \approx 20$ ns [53].

The Hanle curve for a trion state is proved to be more complex than a simple Lorentz contour. Figure 5 displays the dependence of the degree of circular polarization of the radiation of X^- trions in a CdSe/ZnSe QD on the transverse magnetic field [54]. The nonmonotonic field dependence of the polarization indicates the presence of contributions with different half-widths, i.e., with different spin lifetimes. The decrease in polarization in stronger fields is related to the precession of the uncompensated spin of the hole in the trion [55]. The half-width of this curve ($H^h_{1/2} = 70$ mT) yields a hole spin lifetime $T_{sh} = \hbar/\mu_B g_h H_{1/2} \approx 500$ ps. This lifetime virtually coincides with the lifetime of the trion [56], thus meaning that the hole spin lifetime is controlled by recombination, i.e., $\tau_s \gg \tau$. The time τ_s of the hole spin relaxation exceeds 10 ns according to measurements performed in Ref. [56]. The increase in the degree of polarization of radiation in the case of weak fields is paradoxical at first glance, since the precession of electron spin should always result in a depolarization. However, this paradox is easily explodable if we take into account that the electron contribution to the polarization of radiation has a negative sign [52, 53], and the decrease in its absolute magnitude leads to a total increase in polarization. From the half-width of the electron depolarization curve it is possible to determine the spin lifetime $T_{se} = \hbar/\mu_B g_e H^e_{1/2} \approx 14$ ns. It is obvious that this large lifetime can be ascribed only to the spin relaxation of an equilibrium electron, since the spin lifetime of a photoexcited charge carrier is limited by a substantially smaller recombination time. Notice that in a longitudinal magnetic field the time of spin relaxation in a QD, just as in bulk crystals, increases substantially. Below, we shall consider two typical examples of a possible practical application of QDs.

Optically programmable electron spin memory. The large times of spin relaxation of charge carriers in semiconductor QDs can be used for the creation of an optically programmable memory. The principle of its operation was demonstrated in Ref. [57], where a QD was utilized for the creation of an electron spin and its subsequent storage and optical readout. In Fig. 6a, a sample with an ensemble of InGaAs QDs is illuminated with circularly polarized radiation. Upon absorption of a photon by a QD, an electron–hole pair (exciton) is formed. To exclude exchange interaction which destroys spin polarization, a reverse bias is applied perpendicular to the layer of QDs. The electric field ionizes the exciton, throwing out a hole from the QD. The high AlGaAs barrier in this case prevents the ejection of an electron from the QD. After the separation of the charges, the spin-polarized electron is stored in the QD. In a time Δt, the voltage changes in such a way that a hole is injected into the QD, where the hole recombines with the electron. In the experiment, the degree of circular polarization of recombination radiation was measured at various Δt and the dependence obtained was employed to determine the spin relaxation time τ_s. A value obtained in a magnetic field $H = 4$ T was, for example, $\tau_s = 20 \pm 6$ ms. It was shown that due to the spin–orbit interaction the single-phonon scattering processes intermix the Zeeman sublevels and make spin flip possible.

Ultrarapid optical control of electron spin in QDs. One more example of the possible application of QDs is based on the employment of the optical Stark effect [58]. Optical radiation (with a frequency ω and intensity I) detuned from the energy ω_0 of the electron transition by $\Delta\omega = \omega - \omega_0$ induces a shift of the transition energy by $\Delta E = D^2 I/(\omega - \omega_0)\sqrt{\varepsilon/\mu}$, where ε and μ are the permittivity and permeability, respectively. When the QD is induced by circularly polarized light (σ^+), the optical transition is allowed to an exciton sublevel $m_z = +1$ (the wave σ^+ interacts with only one of the sublevels of the Zeeman doublet $m_z = \pm 1$). The Zeeman sublevel $m_z = +1$ undergoes a Stark shift, while the energy of the sublevel $m_z = -1$ remains unchanged, i.e., a splitting arises between the sublevels $m_z = +1$ and $m_z = -1$. This is equivalent to the action of an effective (Stark) magnetic field $H_{Stark} = \Delta E/\mu_B g$ oriented along the wave vector of the photon. Using short light pulses with a sufficiently large intensity makes it possible to rapidly change the spin direction due to the precession in the Stark field. It should be noted that the optical Stark effect upon illumination by circularly polarized light and the appearance of a Stark magnetic field also allow a different interpretation — in terms of the inverse Faraday effect [59, 60]. The optical Stark effect is an illustration of the equivalence of the action of a magnetic field and circularly polarized light.

Notice, however, that for QDs to be used widely in devices, it is necessary that the long spin lifetimes be retained at room temperature, which has not yet been achieved.

6. Spin transport

The spin transport in spin electronics plays a very important role, similar to the charge transfer in conventional electronics. The problems of spin-dependent scattering, spin diffusion, spin transfer through various interfaces, controling spins using an electric field, etc. are in the spotlight of spin physics. The optical orientation (optical injection) is an elegant and efficient method of creating a nonequilibrium

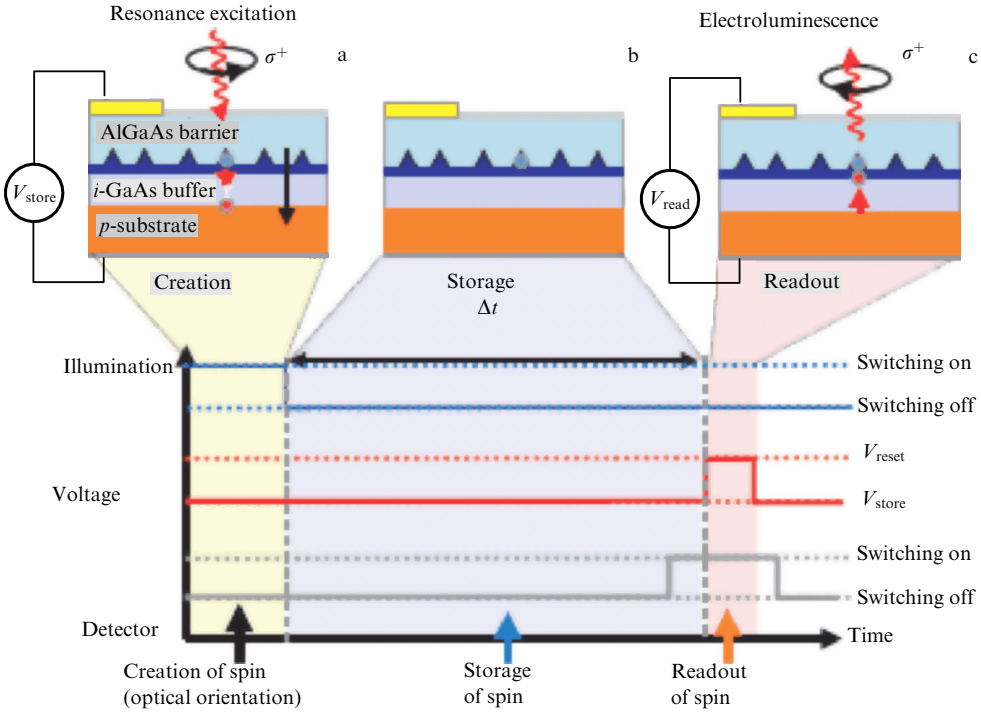

Figure 6. Schematic and the principle of operation of an optically programmable memory (dark triangles correspond to InGaAs QDs): (a) the resonantly excited excitons are ionized in a strong electric field applied to the p-i-n structure (transformation of a photon into a charge). The AlGaAs barrier prevents the escape of the electron from the QD; (b) after the separation of the charges, the spin-polarized electron is stored in the QD, and (c) readout of the electron spin state upon the application of a reverse bias which injects a hole into the QD. Recombination of the hole and electron generates a photon with a polarization that is determined by the electron spin (borrowed from Ref. [57]).

spin, but it is desirable to have a simpler injection technique, which would not require the use of laser sources. Various ways have been suggested, such as passing current through a ferromagnetic contact (*spin injection*) and passing current through a semiconductor (*spin Hall effect, spin generation by electric current*).

Electric spin injection. The idea of the creation of nonequilibrium spin polarization in a semiconductor by passing current through a ferromagnetic contact was suggested by Aronov and Pikus [9]. Because of some specific features of the band structure of a ferromagnet, the conductivities of two groups of electrons with magnetic moments oriented parallel and antiparallel to the magnetization vector are different ($\sigma_{F\uparrow} \neq \sigma_{F\downarrow}$). If electron scattering occurs predominantly without spin flip, the two groups of electrons do not intermix and the current in the ferromagnets proves to be spin-polarized, $I_\uparrow \neq I_\downarrow$, as is illustrated in Fig. 7a. For this condition to be fulfilled, it is necessary that the momentum scattering time τ_{tr} (transport time) be substantially less than the spin relaxation time τ_s, i.e., $\tau_{tr} \ll \tau_s$. In many ferromagnets this condition is satisfied already at room temperature. Upon injection, the spin orientation in a semiconductor exists on a spin diffusion length $L_s = \sqrt{D\tau_s}$ (D is the diffusion coefficient). Alvarado and Renaud in their experimental work [10] realized spin injection into GaAs from a ferromagnetic nickel tip of a scanning tunneling microscope. Later on, it was found that the spin injection in a heterostructure consisting of a ferromagnetic metal and a semiconductor is ineffective [61]. A physical explanation of this problem was given in Refs [62, 63]. Figure 7b displays an equivalent circuit of a ferromagnet/semiconductor contact in the form of a parallel connection of resistances, of a ferromagnet, $R_{F\uparrow} \propto \sigma_{F\uparrow}^{-1}$, $R_{F\downarrow} \propto \sigma_{F\downarrow}^{-1}$, and a semiconductor, R_{SC}. The low spin injection coefficient γ, which is defined as $\gamma = (I_\uparrow - I_\downarrow)/(I_\uparrow + I_\downarrow)$, is caused by the large difference in the conductivities of the contacting materials — metal and semiconductor. Indeed, in view of the inequality $R_{F\uparrow,\downarrow} \ll R_{SC}$, the currents $I_\uparrow$ and $I_\downarrow$ are virtually coincident, which means the absence of spin injection. This problem can be bypassed in two ways: (a) by using a ferromagnetic semiconductor with $R_{F\uparrow,\downarrow} \approx R_{SC}$ as the spin injector, and (b) by using a conventional metallic ferromagnet but with a high contact resistance: $R_c > R_{SC}$ [64]. To achieve the condition $R_c > R_{SC}$, sometimes a tunneling insulating interlayer is deposited between the ferromagnet and semiconductor [65]; in this case, the tunneling current becomes spin-dependent. The success of the first experiment on spin injection was precisely due to the fact that a tunneling microscope was used in it. The spin injection from a ferromagnetic GaMnAs type semiconductor into GaAs was effected in Refs [66, 67].

Spin Hall effect. The effect consists in the appearance of a spin flow in the direction perpendicular to the electric current. The spin flux q_{ij} is proportional to the applied electric field E_k: $q_{ij} = \beta n \varepsilon_{ijk} E_k$, where ε_{ijk} is an asymmetric tensor, β is the spin–orbit interaction constant, and n is the concentration of charge carriers [7]. The spin flow, in turn, leads to an accumulation of the nonequilibrium spin on the sample faces (Fig. 8b). No charge current arises in the transverse direction, and the voltages on the lateral faces of the sample (Hall contacts) are identically equal to zero. However, if the current injected into the sample possesses a spin polarization $\mathbf{P}$ (spin injection), then a charge Hall current $\mathbf{j}_H \propto \beta n \mathbf{E} \times \mathbf{P}$ [7] and the Hall voltage U_H arise in the transverse direction. One of the most important microscopic mechanisms of the spin

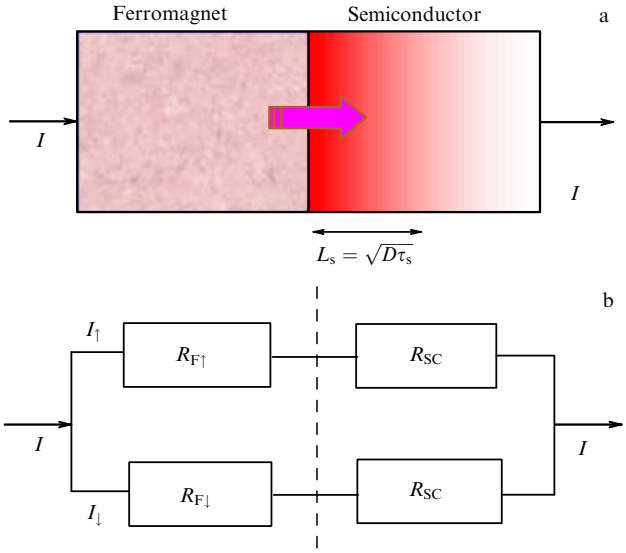

Figure 7. (a) Schematic of a spin injection from a ferromagnetic material into a semiconductor. Spin relaxation in the semiconductor leads to a decrease in the nonequilibrium spin when moving from the boundary. (b) Equivalent circuit of the ferromagnet/semiconductor contact in the form of a parallel connection of resistances. Electrons polarized against the magnetization vector of the ferromagnet flow along the upper part of the circuit; electrons polarized along the magnetization vector pass in the lower part of the circuit. Although $R_{F\downarrow} \neq R_{F\uparrow}$, the current is not polarized: since $R_{F\uparrow,\downarrow} \ll R_{SC}$, the current in the upper ($I_\uparrow$) and lower ($I_\uparrow$) parts of the circuit are almost coincident: $I_\uparrow = U/(R_{F\uparrow} + R_{SC}) \approx U/R_{SC}$, and $I_\downarrow = U/(R_{F\downarrow} + R_{SC}) \approx U/R_{SC}$.

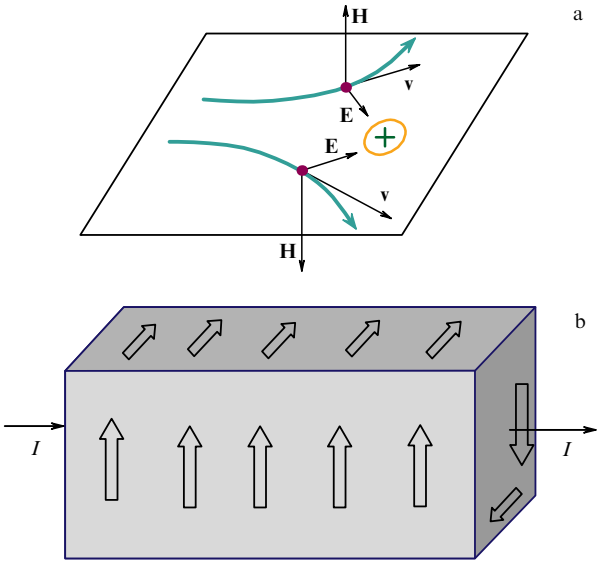

Figure 8. Spin Hall effect: (a) electron scattering on an impurity to the left or to the right. The electron moving with a velocity $\mathbf{v}$ in an electric field $\mathbf{E}$ of the impurity 'feels' the magnetic field $\mathbf{H} = (\mathbf{v} \times \mathbf{E})/c$, where c is the speed of light. The sign of the magnetic field depends on the direction of scattering. (b) The appearance of a spin current perpendicular to the flowing electric current I. On the lateral faces of the sample, a spin polarization appears (double arrows). The region of the existence of spin polarization near the sample surface is determined by the spin diffusion length $L_s = \sqrt{D\tau_s}$.

Hall effect is guided by the asymmetry of electron scattering: due to spin–orbit interaction, electrons with opposite spins scatter predominantly in opposite directions [68] (Fig. 8a). A

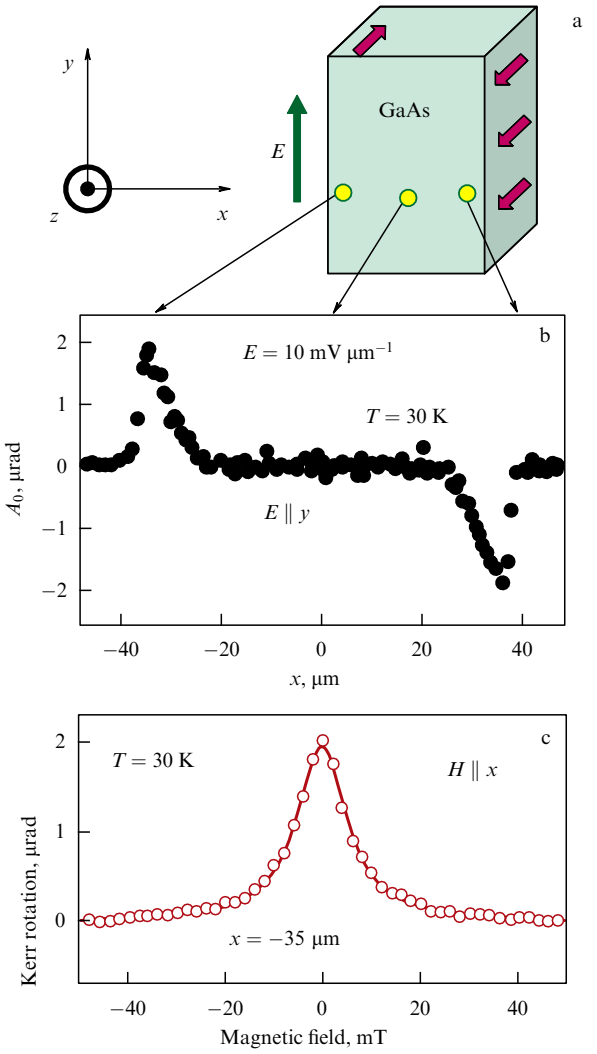

Figure 9. Experimental exposition of a spin Hall effect: (a) Schematic of the experiment. The electric current is passed along the y-axis. (b) The amplitude A_0 of the Kerr rotation on the front surface of the sample is measured depending on the coordinate x. The signal is proportional to the spin projection onto the z-axis. The spatial width of the peaks of Kerr rotation at $x = \pm 35$ μm is determined by the spin diffusion length. (c) Dependence of the signal at $x = -35$ μm on the magnetic field $H \| x$ (circles). The precession in a magnetic field leads to a depolarization of the nonequilibrium spin and a decrease in the Kerr rotation amplitude. The solid line corresponds to the approximation by a Lorentz curve (borrowed from Ref. [66]).

significant feature of the effect is that the contribution to the asymmetry comes only from the spin polarization component perpendicular to the scattering plane: the scattering cross section is proportional to the product $\mathbf{Pn}$, where $\mathbf{n} \propto \mathbf{k} \times \mathbf{k}'$ is the unit vector perpendicular to the scattering plane, and $\mathbf{k}$ and $\mathbf{k}'$ are the electron momenta prior to and after scattering event, respectively. The spin Hall effect was experimentally revealed in 2004 in a thin GaAs film at $T = 30$ K [69]; two years later, the effect was observed at room temperature in films of the ZnSe semiconductor [70]. The spin polarization that accumulated at the sample edges was measured using the magnetooptical method by the rotation angle of the plane of polarization of light reflected from the sample (the Kerr effect). Figure 9a, b displays the schematic of the experiment and the dependence of the signal amplitude on the coordinate along the sample surface. The amplitude of the signal is

proportional to the spin projection onto the z-axis. It may be seen that the amplitude of Kerr rotation near the sample edges, where the spin accumulation occurs, has the opposite sign, and in the middle part of the sample it is equal to zero. At a temperature of 30 K, the magnitude of spin concentration and of the spin Hall conductivity (ratio of the transverse spin current to the strength of an electric field applied along the conductor) in the GaAs film were $n = 16\mu_B\ \mu m^{-3}$ and $\sigma = j_s/E \approx 3\ \Omega^{-1}\,m^{-1}$, respectively. As the temperature increases to room temperature, the spin concentration and the spin Hall conductivity decrease by factors of 10 and 6, respectively, but remain measurable [70].

In Refs [71, 72], the appearance of spin polarization upon passage of an electric current was also predicted. However, the origin of such polarization is related to 'Boltzmann' population of the Zeeman sublevels in the effective magnetic field $H_{\rm eff}$ arising upon the passage of current [38] rather than to electron scattering. In the case of Boltzmann statistics, the spin polarization is proportional to $\mu_B H_{\rm eff}/kT$; in the case of Fermi statistics, it is proportional to $\mu_B H_{\rm eff}/E_F$ (T and E_F are the temperature and the Fermi energy, respectively). This fact was revealed experimentally for the two-dimensional gas of holes in the GaAs/GaAlAs structure in Refs [73, 74], and for the electron gas in Refs [75, 76].

The mechanisms and the manifestations of the spin Hall effect have been described in detail in monograph [14].

Inverse spin Hall effect. An opposite effect also exists: on creating the spin polarization **P**, an electric current $\mathbf{j}/e \propto \delta\,\mathrm{rot}\,\mathbf{P}$ is built up [77]. This effect was observed experimentally in Ref. [78]. The circularly polarized light was absorbed near the surface of the GaAs semiconductor and created polarization **P** and a diffusion current along the z-axis (Fig. 10). Although in this case a gradient of polarization $dP_z/dz \neq 0$ exists, no current arises in the plane of the sample, since $\mathbf{P}\|\mathbf{z}$ and $\mathrm{rot}\,\mathbf{P} = 0$. It is necessary that the spin had a component parallel to the sample plane. Upon application of a magnetic field H_x, the spin precession in a magnetic field leads to the appearance of a y-component of the vector **P**, which gives rise to a nonzero current $\mathbf{j} \propto \mathrm{rot}\,\mathbf{P} \propto \mathbf{e}_x\,dP_y/dz$. Figure 10b demonstrates the voltage U arising at the contacts as a function of the magnetic field strength. The $U(H)$ dependence completely reproduces the $P_y(H)$ dependence. This experiment apparently for the first time demonstrated the principle of the electrical registration of a spin Hall effect.

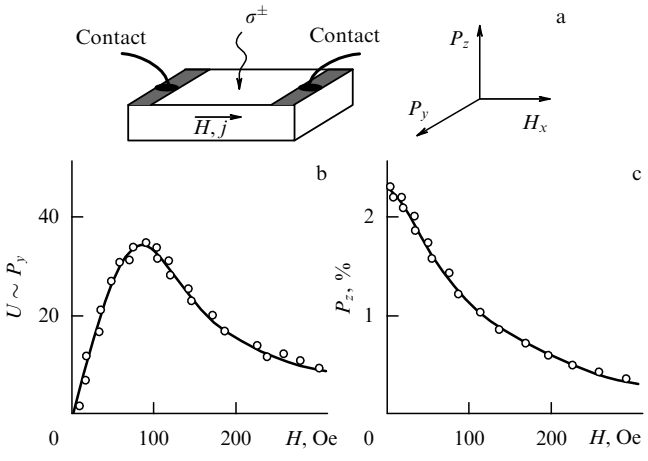

Figure 10. Inverse spin Hall effect. (a) Sample with contacts and the geometry of the experiment; circularly polarized light is absorbed near the surface of the semiconductor and creates spin polarization P_z. (b) In a field H_x, polarization P_y appears, which leads to the appearance of a current and, correspondingly, voltage $U \sim P_y$ at the contacts. (c) Dependence of P_z on the magnetic field $H = H_x$ (Hanle effect) (borrowed from Ref. [75]).

It should be noted that the absorption of circularly polarized light in semiconductors can lead to the appearance of electric current even in the absence of a magnetic field [in the above-considered case (see Fig. 10b), the current arises in a magnetic field]. This phenomenon, known as the *circular photogalvanic effect*, is caused by the asymmetry in the elementary processes of photoexcitation and takes place only in gyrotropic media [79]. The appearance of a current upon uniform illumination of a gyrotropic tellurium crystal by circularly polarized light was first revealed experimentally in Ref. [80]. As was expected, the current direction changed to the opposite one upon inversion of the sign of circular polarization of light. A review of the circular photogalvanic effect in nanostructures is given in [81].

Generation of spin by electric current. Vorob'ev et al. [8] found a change in the angle of rotation of the plane of polarization of linearly polarized light upon passage of electric current through a gyrotropic tellurium crystal. The angle of the additional rotation is proportional to the current and changes sign when the current direction changes (Fig. 11). The light propagated along the C_3-axis of tellurium (the crystal symmetry is D_3). The origin of the effect is explained in Fig. 11b, where the tellurium band structure is shown. A strong spin–orbit interaction in the valence band leads to a mutual shift in the k space of subbands with the projections $J_z = \pm 3/2$ of the angular momentum. As a result, the valence band becomes double-humped, so that the extremum of the subband $J_z = +3/2$ proves to be at the point $k_z = +k_0$, and the extremum $J_z = -3/2$ at the point $k_z = -k_0$. The electric field $E = E_z$ is responsible for a breaking of the symmetry of the distribution function relative to k_z, inducing the predominant population of hole states with $J_z = +3/2$, i.e., the polarization of hole spins. This automatically results in a change in the probabilities of interband transitions (absorption and refraction) for the circularly polarized components σ^+ and σ^-. Notice especially the large magnitude of the effect (compared to other spin effects): for a current $j = 700$ A cm^{-2}, the angle of rotation of the plane of polarization is $\varphi = 2.5 \times 10^{-2}$ rad. Let us recall that the magnitude of the Kerr angle in the spin Hall effect reaches only several microradians. The possibility of changing the angle of rotation of the polarization plane by passing current was predicted in Ref. [82].

7. Spintronics

The goal of spintronics lies in the employment of fundamental knowledge in the field of spin-dependent phenomena for the development (creation) of devices for storage and processing of information. In recent years, metallic spintronics has demonstrated impressive successes [83]. However, the fundamental impossibility of the amplification of electrical signals strongly limits the potential of metallic spintronics. No metallic analog of a bipolar transistor exists, in which the base current would be accompanied by a multiply amplified collector–emitter current. Semiconductor spintronics is called upon to integrate the best qualities of the two systems that exist so far independently — semiconductor logic and magnetic memory. The possible line of studies in this way involves

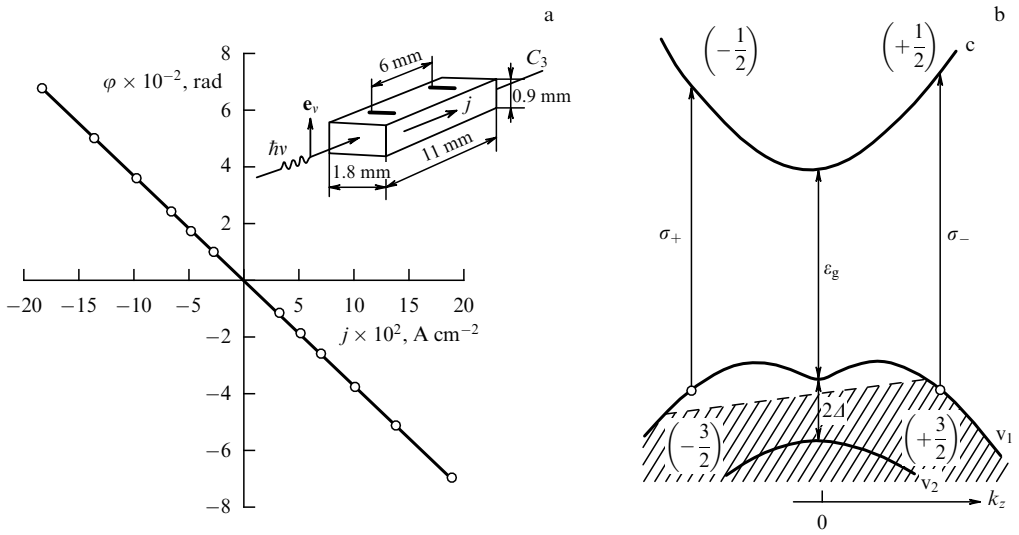

Figure 11. Generation of spin by an electric current. (a) Dependence of the additional angle of rotation φ of the plane of light polarization on the current density in tellurium with a hole concentration $n_h = 1.5 \times 10^{17}$ cm^{-3} at a temperature of 77 K. The current flows along the symmetry axis C_3 of the gyrotropic crystal; the linearly polarized light propagates along the same axis. (b) Band structure of tellurium: c, conduction band; v_1 and v_2, the valence bands; dashed line, the Fermi level of holes in an electric field. The subbands with the projections $J_z = +3/2$ and $J_z = -3/2$ of the angular momentum are shifted in the k space (borrowed from Ref. [8]).

the development of new hybrid semiconductor/ferromagnet devices, which can play the role of both a logic and a memory component and can be produced within the same technology. The advantages of spintronics are the nonvolatility, small leakage currents, small switching energy, and high operation speed. A high speed of operation of spintronics devices can be achieved since it is by no means necessary to transfer in space a charge and related mass. To switch a state it is sufficient to change the spin state (to rotate the spin).

The necessary conditions for a successful realization of the ideas of semiconductor spintronics can be formulated as follows.

(1) In spintronic devices, spin-polarized carriers are used; this means that a source of spin-polarized carriers is necessary. This problem can be solved by injection of carriers from a ferromagnetic material into a semiconductor or, alternatively, a ferromagnetic semiconductor can be employed, in which an equilibrium spin polarization of intrinsic carriers exists. Such a ferromagnetic semiconductor should have a Curie point above room temperature, possess a high mobility of carriers, and allow creation of regions with n and p conductivities in the same crystal.

(2) Spin-polarized carriers should be transferred through an interface between different semiconductor materials or over a certain distance inside the semiconductor without loss of polarization, i.e., a large spin diffusion length is required.

(3) The spin lifetime should be sufficiently large, in order to allow the desired operations to be performed. Since the materials of both n and p types are expected to be used in spintronics devices, these requirements refer to materials with both conductivity types.

(4) The possibility of controling the spin state of an electron using external fields, especially an electric field, is desirable.

The problem of integration can mainly be solved by utilizing ferromagnetic semiconductors with good electric and magnetic characteristics. The difficulty is only that no ferromagnetic semiconductors with satisfactory properties exist so far. One of the potential candidates for such materials is gallium arsenide doped with manganese. It is believed that the local magnetic momenta of Mn atoms orient spins of mobile holes that are formed upon substitution of manganese for gallium. However, the introduction of a sufficient concentration of manganese atoms impairs the electrophysical characteristics of the material. This is explained by a worsening of the perfection of the samples: the mean free path of carriers in them does not usually exceed 10 Å. In addition, the Curie temperature in GaAs:Mn does not exceed 150 K, which is still quite far from room temperature [88].

In connection with the first condition above, a question arises: is ferromagnetism a prerequisite component of semiconductor spintronics? The use of a spin–orbit interaction for the generation and detection of spins makes it possible to avoid the necessity of using a ferromagnet and the difficulties related to the introduction of local magnetic fields into the architecture of spin devices. As we saw in Sections 3 and 6, in many cases the spin polarization in semiconductors can be created and detected optically or electrically. Unfortunately, the effects induced by spin–orbit interactions are mostly weak, and are noticeable only at low temperatures. Therefore, no concrete devices have yet been created on their basis. At present, an important problem is the search for and the investigation of new materials in which these effects would be sufficiently strong and could be observed at room temperature.

Spin transistor. In 1990, a device was suggested which was called by the authors an analog of an electrooptical modulator [11] (this name correctly reflects the essence of the device). This invention, which is more widely known under the name of spin transistor, made a powerful impact on fundamental and applied investigations in spintronics, although to date it has not found a real practical application. This device resembles a field-effect transistor: it has a source, a drain, and a two-dimensional channel with controllable conductivity. The source and drain, as distinct from those in an ordinary transistor, are formed from a ferromagnetic metal (Fe) and serve as a polarizer and analyzer of an

electron spin. The first injects polarized carriers into a two-dimensional layer, while the second determines the transmission of the device, since the current depends on the mutual orientation of the average spin of electrons and the drain magnetization. The electron moving in a two-dimensional channel feels the effective Rashba field, and its spin turns by a certain angle. When a voltage is applied across the gate of the transistor, the Rashba constant α changes, which leads to a change in the angle of rotation and, consequently, in the current. The electron scattering in the channel results in an intermixing of spin states; therefore, the above-described spin transistor can operate successfully only in the ballistic regime.

The authors of Ref. [84] suggested a 'nonballistic' version of a spin transistor, in which the possibility of changing the relative Dresselhaus and Rashba interactions is used. In particular, at $\alpha = \beta$ the spin wave function is independent of the particle momentum and the spin is retained upon scattering. The device operates as follows. In the initial (switched-off) state, $\alpha \neq \beta$, and the injected spins are depolarized as a result of scattering before they reach the drain. The current in this case is equal to half the maximum possible current that is realized in the case of the parallel orientation of the electron spin and drain magnetization. Then, such a voltage is applied across the gate, which ensures the equality of the Dresselhaus and Rashba contributions, i.e., $\alpha = \beta$. In this (switched-on) state, the electron scattering does not lead to spin relaxation and the electron spin is transferred from the source to the drain without loss. It is obvious that the current passing through the device in this case (under the assumption of the parallel magnetization of the ferromagnetic contacts) will be maximum. It is also readily seen that the current can be modulated by switching over between two states, $\alpha = +\beta$ and $\alpha = -\beta$, by applying appropriate voltages on the gate. The experimental realization of a spin transistor on the basis of a two-dimensional gas with a high mobility in InAs operating at a temperature of 1.8 K is reported in Ref. [85]. The problems that are solved using a spin transistor can also be solved using ordinary field-effect transistors, without involving electron spins. The main advantage of a spin transistor lies in the fact that the leakage currents and the switching energy can be made substantially less than in existing and future complementary metal–oxide–semiconductor (CMOS) transistors. A critical review of the various versions of spin transistors is given in Ref. [86].

Quantum calculations. The spin degrees of freedom can be utilized for the organization of quantum calculations. A quantum particle which, as opposed to a classical particle, can reside in a superposition state represents a quantum bit of information or *qubit* — a quantum analog of a classical bit. The most common example of a qubit is an electron spin in the state representing a superposition of basis states $-1/2$ and $+1/2$. For the organization of quantum calculations with spin qubits, materials with large times of spin relaxation are required. The lifetime of a spin should be greater than the time necessary for the performance of quantum operations with it (spatial rotations of spin in an effective or in an external magnetic field, and readout of information). It is assumed that the time of one operation with quantum qubits reaches approximately 1 ns. Consequently, to perform several operations, a time on the order of 10 ns or greater is required.

Spin states of electrons in a QD can be considered as probable candidates for the logic states of quantum bits. For example, an excess electron that occupies a size-quantized energy level in the conduction band of a semiconductor QD (an 'artificial atom') represents one qubit, while a pair of such QDs (an 'artificial molecule') is already a two-qubit system. Operations with such a system can be realized by controlling the exchange interaction between electrons using electric pulses. An electron spin in a QD can also be readout and initiated optically [87]. The absorption of a photon in a QD that contains an electron leads to the formation of a trion $|J_z, S_z, S'_z\rangle$, where J_z, S_z, and S'_z are the projections of the spins of the hole and of two electrons in the trion. If in the initial state the electron in the QD has a spin projection $S'_z = +1/2$ ($S'_z = -1/2$), the transition with the absorption of a σ^+ photon (σ^- photon) and the formation of a trion $|+3/2, -1/2, +1/2\rangle$ ($|-3/2, +1/2, -1/2\rangle$) is allowed. The recombination in these states is accompanied by the emission of a σ^+ or a σ^- photon, i.e., it is unambiguously determined by the projection S'_z of the electron spin in the initial state, which makes it possible to readout the spin state of the electron.

For the creation of memory modules and logic devices, it is also suggested to use the spin of lattice nuclei. One of the ideas consists in utilizing electron spin as a 'bus' for the transfer of data into the nuclei (through contact interaction), where these data could be processed or stored. The readout is also performed using an electron spin localized at an impurity center (defect) or in a QD. The advantage of the nuclear spin is that the nuclear polarization is retained for a long time (several days or weeks, depending on temperature). In Refs [88, 89], various types of constructions of quantum computers on the basis of QDs were suggested.

Equilibrium spin and spintronics. The employment of spins in the devices of semiconductor spintronics, as was already noted above, requires long spin lifetimes. At room temperature, the nonequilibrium spin is unstable — it decays in a short time (10–100 ps). To bypass this difficulty, it is necessary to learn to use an equilibrium spin. It is attractive to apply the so-called *proximity effect* in a hybrid ferromagnet (FM)–semiconductor system. If the FM is sufficiently close to the electronic system of the semiconductor, an exchange coupling of their spin systems occurs. The unique feature of such a coupled system is the possibility of separating functions of storage and controlling: the storage of the spin occurs in the ferromagnet, while the controlling of the spin can be organized utilizing the semiconductor.

In Ref. [90], an exchange coupling of an FM with a two-dimensional hole gas (2DHG) was considered (Fig. 12) and a principle for the switching-over of the magnetization of a ferromagnetic film deposited onto a semiconductor was established [90, 91]. The heart of the suggestion is as follows. The ground state of a hole in the valence band corresponds to heavy holes, whose angular momentum $J = 3/2$ is connected with the direction of the normal (z-axis) to the QW. For this reason, the exchange interaction of 2D holes with the magnetic atoms of the ferromagnet is anisotropic [92]. The exchange energy per unit surface area is proportional to the product of the z-component $\langle J_z \rangle$ of the average spin of holes and the z-component of the unit vector $\mathbf{m}$ oriented along the magnetization vector $\mathbf{M}$: $E_{\text{ex}} = -Anm_z\langle J_z \rangle$, where A is the exchange constant, and n is the surface concentration of holes. The exchange interaction (the exchange field of the ferromagnet, H_{FM}) splits the state of the hole with $J_z = \pm 3/2$ by a magnitude $A \sim 0.1$ eV; as a result, the holes become polarized. Those holes polarized along the z-axis, in turn, create an exchange field $H_{\text{h}z}$ tending to orient the magnetization of the ferromagnet along the normal and to decrease the

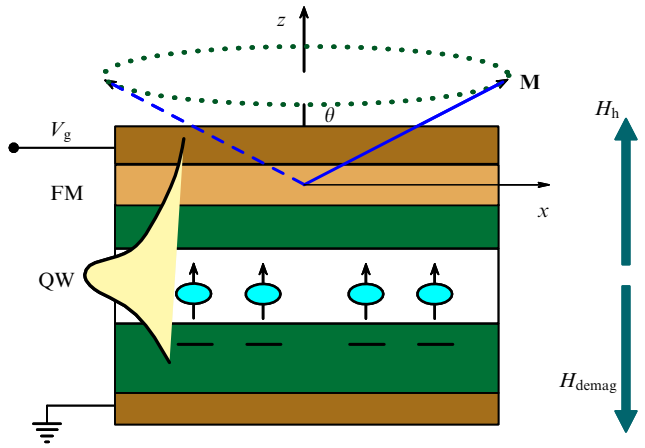

Figure 12. Schematics of a structure that ensures a dynamic switching of magnetization on the basis of the proximity effect. The quantum well (QW) is separated from the ferromagnetic layer (FM) by a thin barrier. On the top, a thin semitransparent layer of metal is applied, which is used for controling the exchange coupling of the holes (dots) and the FM. Upon application of voltage, the holes are either attracted to the metal or repulsed from it (an adapted figure borrowed from Ref. 87]).

exchange energy E_{ex}. According to Ref. [91], the exchange field is $H_{hz} = An\langle J_z\rangle/Md$ (where d is the film thickness). However, the deflection of the vector **M** from the film plane is accompanied by the appearance of a demagnetizing field of strength $H_{demag} = -4\pi M_z$ ($H_{demag} \sim 1$ kOe). In the equilibrium state, the magnetization is oriented at a certain angle θ to the z-axis, so that the demagnetizing field is balanced by the exchange field. Thus, the magnetization of the FM is controlled by the anisotropic exchange interaction with holes. It is obvious that the magnitude of the exchange coupling depends on the spacing between the FM and the holes. A voltage V_g applied to the gate (see Fig. 12) attracts or repulses holes, changing the strength of the exchange coupling with the ferromagnet. By applying a positive potential across the gate, the exchange field of holes can be decreased (ideally, removed completely). Then, the magnetization **M**, which makes an angle θ with the field H_{demag}, starts precessing about it. At a definite duration of the electric-field pulse, the magnetization rotates by 180°. Thus, the dynamic controling of the ferromagnet magnetization can be effected using a related exchange-coupled semiconductor QW. The advantage of such a scheme lies in the fact that the device can operate at room temperature (with an appropriate choice of a ferromagnet [91]).

Experimentally, the exchange coupling of a ferromagnetic semiconductor GaAs:Mn with the holes in an adjacent GaAs QW was observed in Ref. [93]. The exchange interaction with an FM induces an equilibrium polarization of holes in the QW, which can be observed from the circular polarization of the luminescence from a QW placed in a magnetic field. An electric field applied perpendicular to the QW plane induces deformation of the wave function of the hole, moving it closer to or farther from the FM layer. The measurements showed that the degree of the circular polarization of the luminescence from the QW depends on the applied electric field.

It should be noted that the electrical switching of magnetization (recording information) is one of the most important technical problems of spintronics (the second part of this problem — the electrical readout of information in the form of the ferromagnet magnetization — has been solved using the giant magnetoresistance effect). Such a switching over is performed relatively easily in FMs based on dilute magnetic semiconductors. Since ferromagnetism in dilute magnetic semiconductors is caused by indirect exchange interaction, which is effected by holes, the change in their concentration leads to a change in the Curie temperature. In Ref. [94], H Ohno and colleagues have demonstrated electrical control of the magnetization of the ferromagnetic layer in an InAs/InMnAs structure. As an electric potential was applied to the gate, the hysteresis loop was changed, which caused the authors to link this with the change in the hole concentration in an InMnAs layer. The results of experiments can also be easily interpreted in terms of the proximity effect [90].

8. Conclusions

To date, numerous new spin-dependent effects have been discovered in semiconductors and hybrid structures with magnets, and a large number of new devices based on them have been suggested. Methods of generation, control, and detection of spins have been developed; they represent the basis of the operation of future spintronic devices. Ferromagnets based on semiconducting III–V compounds have been synthesized and studied comprehensively. At the same time, no concrete applications of spin phenomena in semiconductors are known so far. The difficulties are connected with the large rate of spin relaxation of electrons in semiconductors and with the absence of ferromagnetic semiconductors at room temperature. A solution to the problem of electron spin relaxation was outlined in Refs [33, 34]. Ferromagnetic semiconductors have a good potential for practical applications in view of the easy control of their magnetization. However, their quality is insufficient so far: FM semiconductors are characterized by a high concentration of defects, inhomogeneity, and a low mobility of carriers. As an alternative, hybrid systems of semiconductors with metallic or insulating ferromagnets can be used. It is just in such hybrid systems that spin phenomena can find application in semiconductors in the nearest future. But many technological difficulties related to the presence of defects at interfaces, the formation of specific interface layers, etc. should first be overcome.

A specific feature of many spin-dependent effects is their smallness. For example, the spin Hall effect is weak because of the smallness of spin–orbit coupling. It seems expedient to make efforts to search and investigate new materials and structures with the given properties and symmetry that will make it possible to obtain the desired spin effects. Methods for the calculation of such structures and for the prediction of their properties and quantitative computation of their parameters should be developed. As an example of a material in which the effect (rotation of the plane of light polarization) manifests itself sufficiently strongly, crystalline tellurium with its unique band structure can be mentioned.

At present, spin-related phenomena are investigated actively not only in semiconductors, but also in metals, insulators, and organic materials. Among the latest studies, investigations of the possibility of using spins of the defects in diamond [the so-called 'nitrogen-vacancy' (NV) defects] for the storage and processing of quantum information should be mentioned. A doubtless advantage of this system is that NV defects possess a large time of spin relaxation at room temperature [95, 96].

The success in the field of metallic spintronics, as well as a deep understanding of the physics of spin processes in semiconductors and hybrid systems with ferromagnets, gives grounds to hope for rapid progress in semiconductor spintronics.

References

1. Hanle W T *Z. Phys.* **30** 93 (1924)
2. Wood R W, Ellett A *Phys. Rev.* **24** 243 (1924)
3. Kastler A *Science* **158** 214 (1967)
4. Lampel G *Phys. Rev. Lett.* **20** 491 (1968)
5. Parsons R R *Phys. Rev. Lett.* **23** 1152 (1969)
6. Meier F, Zakharchenya B P (Eds) *Optical Orientation* (Amsterdam: North-Holland, 1984) [Translated into Russian (Leningrad: Nauka, 1989)]
7. D'yakonov M I, Perel V I *Pis'ma Zh. Eksp. Teor. Fiz.* **13** 206 (1971) [*JETP Lett.* **13** 144 (1971)]
8. Vorob'ev L E et al. *Pis'ma Zh. Eksp. Teor. Fiz.* **29** 485 (1979) [*JETP Lett.* **29** 441 (1979)]
9. Aronov A G, Pikus G E *Fiz. Tekhn. Poluprovodn.* **10** 1177 (1976) [*Sov. Phys. Semicond.* **10** 698 (1976)]
10. Alvarado S F, Renaud P *Phys. Rev. Lett.* **68** 1387 (1992)
11. Datta S, Das B *Appl. Phys. Lett.* **56** 665 (1990)
12. The Discovery of Giant Magnetoresistance (Scientific Background on the Nobel Prize in Physics 2007), http://www.kva.se/Documents/Priser/Nobel/2007/sciback_fy_en_07.pdf
13. Kusrayev Yu G, Landwehr G (Eds) *Semicond. Sci. Technol.* **23** (11) (2008), Special Issue "Optical Orientation"
14. Dyakonov M I (Ed.) *Spin Physics in Semiconductors* (Berlin: Springer, 2008)
15. Elliott R J *Phys. Rev.* **96** 266 (1954)
16. Dresselhaus G *Phys. Rev.* **100** 580 (1955)
17. D'yakonov M I, Perel' V I *Fiz. Tverd. Tela* **13** 3581 (1971) [*Sov. Phys. Solid State* **13** 3023 (1971)]
18. Bir G L, Aronov A G, Pikus G E *Zh. Eksp. Teor. Fiz.* **69** 1382 (1975) [*Sov. Phys. JETP* **42** 705 (1975)]
19. Fishman G, Lampel G *Phys. Rev. B* **16** 820 (1977)
20. Crooker S A et al. *Phys. Rev. B* **56** 7574 (1997)
21. Akimoto R et al. *Phys. Rev. B* **57** 7208 (1998)
22. Camilleri C et al. *Phys. Rev. B* **64** 085331 (2001)
23. Bastard G, Chang L L *Phys. Rev. B* **41** 7899 (1990)
24. Abragam A *The Principles of Nuclear Magnetism* (Oxford: Clarendon Press, 1961) [Translated into Russian (Moscow: IL, 1963)]
25. D'yakonov M I, Perel' V I *Zh. Eksp. Teor. Fiz.* **65** 362 (1973) [*Sov. Phys. JETP* **38** 177 (1973)]
26. Merkulov I A, Efros Al L, Rosen M *Phys. Rev. B* **65** 205309 (2002)
27. Dzhioev R I et al. *Phys. Rev. B* **66** 245204 (2002)
28. Kavokin K V *Phys. Rev. B* **64** 075305 (2001)
29. Astakhov G V et al. *Phys. Rev. Lett.* **101** 076602 (2008)
30. Karlik I Ya et al. *Fiz. Tverd. Tela* **24** 3550 (1982) [*Sov. Phys. Solid State* **24** 2022 (1982)]
31. Akimov I A et al. *Phys. Rev. B* **80** 081203(R) (2009)
32. Lombez L et al. *Appl. Phys. Lett.* **87** 252115 (2005)
33. Kalevich V K et al. *Physica B* **404** 4929 (2009)
34. Kalevich V K et al. *Pis'ma Zh. Eksp. Teor. Fiz.* **85** 208 (2007) [*JETP Lett.* **85** 174 (2007)]
35. Bychkov Yu A, Rashba E I *J. Phys. C* **17** 6039 (1984)
36. Dyakonov M I, Kachorovskii V Yu *Fiz. Tekh. Poluprovod.* **20** 178 (1986) [*Sov. Phys. Semicond.* **20** 110 (1986)]
37. Averkiev N S *Usp. Fiz. Nauk* **180** 785 (2010) [*Phys. Usp.* **53** 742 (2010)]
38. Kalevich V K, Korenev V L *Pis'ma Zh. Eksp. Teor. Fiz.* **52** 859 (1990) [*JETP Lett.* **52** 230 (1990)]
39. Khaetskii A V, Nazarov Yu V *Phys. Rev. B* **61** 12639 (2000)
40. Woods L M, Reinecke T L, Lyanda-Geller Y *Phys. Rev. B* **66** 161318(R) (2002)
41. Paillard M et al. *Phys. Rev. Lett.* **86** 1634 (2001)
42. Dzhioev R I et al. *Pis'ma Zh. Eksp. Teor. Fiz.* **65** 766 (1997) [*JETP Lett.* **65** 804 (1997)]
43. Ivchenko E L, Pikus G E *Superlattices and Other Heterostructures. Symmetry and Optical Phenomena* (Berlin: Springer-Verlag, 1995)
44. Lavallard P, Gourdon C, Planel R *Superlattices Microstruct.* **12** 321 (1992)
45. van Kesteren H W et al. *Phys. Rev. B* **41** 5283 (1990)
46. Tartakovskii A I et al. *Phys. Rev. Lett.* **93** 057401 (2004)
47. Ivchenko E L *Phys. Status Solidi A* **164** 487 (1997)
48. Kusrayev Yu G et al. *Phys. Rev. B* **72** 155301 (2005)
49. Koudinov A V et al. *Phys. Rev. B* **78** 045309 (2008)
50. Bayer M et al. *Phys. Rev. B* **65** 195315 (2002)
51. Finley J J et al. *Phys. Rev. B* **66** 153316 (2002)
52. Bracker A S et al. *Phys. Rev. Lett.* **94** 047402 (2005)
53. Dzhioev R I et al. *Phys. Rev. B* **66** 153409 (2002)
54. Kusrayev Yu G *Semicond. Sci. Technol.* **23** 114013 (2008)
55. Kusrayev Yu G et al. *Phys. Rev. B* **76** 153307 (2007)
56. Flissikowski T et al. *Phys. Rev. B* **68** 161309(R) (2003)
57. Kroutvar M et al. *Nature* **432** 81 (2004)
58. Berezovsky J et al. *Science* **320** 349 (2008)
59. Pitaevskii L P *Zh. Eksp. Teor. Fiz.* **39** 1450 (1960) [*Sov. Phys. JETP* **12** 1008 (1961)]
60. Landau L D, Lifshitz E M *Elektrodinamika Sploshnykh Sred* (Electrodynamics of Continuous Media) (Moscow: Nauka, 1982) [Translated into English (Oxford: Pergamon Press, 1983)]
61. Filip A T et al. *Phys. Rev. B* **62** 9996 (2000)
62. Johnson M, Silsbee R H *Phys. Rev. Lett.* **55** 1790 (1985)
63. Schmidt G et al. *Phys. Rev. B* **62** R4790 (2000)
64. Rashba E I *Phys. Rev. B* **62** R16267 (2000)
65. Motsnyi V F et al. *Appl. Phys. Lett.* **81** 265 (2002)
66. Ohno Y et al. *Nature* **402** 790 (1999)
67. Mattana R et al. *Phys. Rev. Lett.* **90** 166601 (2003)
68. Mott N F *Proc. R. Soc. London A* **124** 425 (1929)
69. Kato Y K et al. *Science* **306** 1910 (2004)
70. Stern N P et al. *Phys. Rev. Lett.* **97** 126603 (2006)
71. Aronov A G, Lyanda-Geller Yu B *Pis'ma Zh. Eksp. Teor. Fiz.* **50** 398 (1989) [*Sov. Phys. JETP* **50** 431 (1989)]
72. Edelstein V M *Solid State Commun.* **73** 233 (1990)
73. Silov A Yu et al. *Appl. Phys. Lett.* **85** 5929 (2004)
74. Ganichev S D et al. *J. Magn. Magn. Mater.* **300** 127 (2006)
75. Sih V et al. *Nature Phys.* **1** 31 (2005)
76. Kato Y K et al. *Phys. Rev. Lett.* **93** 176601 (2004)
77. Averkiev N S, Dyakonov M I *Fiz. Tekh. Poluprovodn.* **17** 629 (1983) [*Sov. Phys. Semicond.* **17** 393 (1983)]
78. Bakun A A et al. *Pis'ma Zh. Eksp. Teor. Fiz.* **40** 464 (1984) [*JETP Lett.* **40** 1293 (1984)]
79. Sturman B I, Fridkin V M *Fotogal'vanicheskii Effekt v Sredakh bez Tsentra Simmetrii i Rodstvennye Yavleniya* (The Photovoltaic and Photorefractive Effects in Noncentrosymmetric Materials) (Moscow: Nauka, 1992) [Translated into English (Philadelphia: Gordon and Breach, 1992)]
80. Asnin V M et al. *Pis'ma Zh. Eksp. Teor. Fiz.* **28** 80 (1978) [*JETP Lett.* **28** 74 (1978)]
81. Ivchenko E L *Usp. Fiz. Nauk* **172** 1461 (2002) [*Phys. Usp.* **45** 1299 (2002)]
82. Baranova N B , Bogdanov Yu V, Zel'dovich B Ya *Usp. Fiz. Nauk* **123** 349 (1977) [*Sov. Phys. Usp.* **20** 870 (1977)]
83. Fert A *Rev. Mod. Phys.* **80** 1517 (2008); *Usp. Fiz. Nauk* **178** 1336 (2008)
84. Schliemann J, Egues J C, Loss D *Phys. Rev. Lett.* **90** 146801 (2003)
85. Koo H C et al. *Science* **325** 1515 (2009)
86. Bandyopadhyay S, Cahay M *Appl. Phys. Lett.* **85** 1433 (2004)
87. Shabaev A et al. *Phys. Rev. B* **68** 201305(R) (2003)
88. Loss D, DiVincenzo D P *Phys. Rev. A* **57** 120 (1998)
89. Burkard G, Loss D, DiVincenzo D P *Phys. Rev. B* **59** 2070 (1999)
90. Korenev V L *Pis'ma Zh. Eksp. Teor. Fiz.* **78** 1053 (2003) [*JETP Lett.* **78** 564 (2003)]
91. Zakharchenya B P, Korenev V L *Usp. Fiz. Nauk* **175** 629 (2005) [*Phys. Usp.* **48** 603 (2005)]
92. Merkulov I A, Kavokin K V *Phys. Rev. B* **52** 1751 (1995)
93. Myers R C, Gossard A C, Awschalom D D *Phys. Rev. B* **69** 161305(R) (2004)
94. Ohno H et al. *Nature* **408** 944 (2000)
95. Gaebel T *Nature Phys.* **2** 408 (2006)
96. Jelezko F et al. *Appl. Phys. Lett.* **81** 2160 (2002)

PACS numbers: **75.76.+j**, **78.56.–a**, **85.75.–d**
DOI: 10.3367/UFNe.0180.201007i.0773

Spin photocurrents in semiconductors

S A Tarasenko

1. Introduction. Phenomenological description

The possibility of efficiently controling spin states of electrons, holes, and other quasiparticles in low-dimensional structures is a key problem in semiconductor spintronics. Owing to spin–orbit interaction, the spin state of a quasiparticle can be changed by affecting its orbital motion. One vivid manifestation of spin–orbit interaction is the spin Hall effect, i.e., the appearance of a transverse spin flow on passing an electric current [1–4]. The spin Hall effect shows itself in semiconductors with free charge carriers as a result of the spin-dependent scattering of carriers on impurities or phonons; it can also be caused by a spin–orbit splitting of electronic states. The spin currents induced by an electric field can also arise during the ballistic transport of electrons, for instance, in tunneling structures. In the last case, the effect is related to the dependence of the tunneling transparency of the potential barrier on the mutual orientation of the electron spin and wave vector [5, 6].

In noncentrosymmetric semiconductor structures, the spin currents can be induced by optical methods [7, 8]. In this case, the generation of a pure spin current, i.e., of a flow of spins without a transfer of an electric charge, is possible. Such a situation corresponds to a nonequilibrium distribution, at which the electrons with a fixed spin orientation move predominantly in one direction and an equal number of particles with the opposite spin move in the opposite direction. The pure spin currents result in a spatial separation of carriers with opposite spin orientations and, in particular, in the emergence of spin polarization near the edges of the sample.

A flux of spins (or, in the general case, a flux of angular momenta) is described by a second-rank pseudotensor J whose components J_β^α correspond to the flux of spins oriented along the α-axis in the direction β; here, α and β are the Cartesian coordinates. In the regime that is linear in light intensity I, the polarization dependence of the components of the spin current is given by the following phenomenological relation:

$$J_\beta^\alpha = I\sum_{\gamma\delta} Q_{\alpha\beta\gamma\delta}\, e_\gamma e_\delta^* + I\sum_{\nu\gamma\delta} D_{\alpha\beta\nu\gamma\delta}\, q_\nu\, e_\gamma e_\delta^*, \qquad (1)$$

where $\mathbf{e}$ is the unit complex vector of light polarization, and $\mathbf{q}$ is the wave vector of the photon. The tensor Q describes spin currents whose components are determined by the light polarization and spatial symmetry of the crystal; Q is nonzero only in noncentrosymmetric media. The tensor D is responsible for the possible contributions to the spin current connected with the transfer of photon momenta to the electron system; in this paper, we neglect these contributions. The absorption of circularly polarized light in semiconductors usually leads to the emergence of a significant spin polarization of photoexcited carriers [9], which hampers the observation of pure spin currents. Therefore, we shall consider spin currents induced by linearly polarized light and assume that the vector $\mathbf{e}$ is real. In this case, the polarization dependence of the spin current components is described by the phenomenological relation (1) in which the tensor Q is symmetrical in the last two indices. A detailed symmetry-based analysis of spin photocurrents in bulk semiconductors and quantum wells grown along different crystallographic directions is given in paper [10].

2. Direct optical transitions in quantum wells

The effect of the generation of spin currents in direct interband or intersubband optical transitions under the influence of linearly polarized light is related to spin-dependent terms that are odd in the wave vector $\mathbf{k}$ in the spectrum of quasiparticles or in the probabilities of optical transitions. These mechanisms can be most vividly explained through the example of optical transitions from the subband of heavy holes (hh1) to the electron subband (e1) in quantum wells grown from semiconductors with a zincblende type lattice along the direction $z' \parallel [110]$.

In quantum wells with the (110) orientation, the effective Hamiltonians describing the states in the conduction band Γ_6 and in the valence band Γ_8 contain contributions that are proportional to $\sigma_{z'}k_{x'}$ and to $J_{z'}k_{x'}$, respectively. Here, $\sigma_{z'}$ is the Pauli matrix; $J_{z'}$ is a matrix with a 4×4 dimension corresponding to the angular momentum 3/2, and $x' \parallel [1\bar{1}0]$ and $y' \parallel [00\bar{1}]$ are the coordinates in the plane of the interfaces. A spin–orbit interaction of this type gives rise to a splitting of the electron subband e1 into branches with spin projections $|\pm 1/2\rangle$, and of the hole subband hh1 into branches $|\pm 3/2\rangle$ (Fig. 1). The selection rules [9] allow only transitions $|+3/2\rangle \to |+1/2\rangle$ and $|-3/2\rangle \to |-1/2\rangle$, which are shown by vertical arrows in Fig. 1. Upon excitation by linearly polarized light, the intensities of both processes coincide; therefore, the average spin of photoelectrons is equal to zero. However, because of the splitting of the subbands e1 and hh1 that is linear in the wave vector, the electrons with a fixed spin orientation are produced with a nonzero average velocity in the plane of the quantum well [8]. Such an asymmetry of the photoexcitation leads to the appearance of an electron flux $\mathbf{i}_{\pm 1/2}$ inside each spin subband. The fluxes $\mathbf{i}_{\pm 1/2}$ are equal in magnitude but are directed oppositely; therefore, this distribution of electrons in the momentum and spin spaces corresponds to a pure spin current.

Under the conditions of a stationary excitation, the density of the spin current in the subband e1 has the form

$$J_{x'}^{z'} = \frac{\gamma_{z'x'}^{(\mathrm{e1})} m_\mathrm{e} + \gamma_{z'x'}^{(\mathrm{hh1})} m_\mathrm{h}}{2\hbar(m_\mathrm{e}+m_\mathrm{h})}\left(\tau_\mathrm{e} + \tilde{\varepsilon}\,\frac{\mathrm{d}\tau_\mathrm{e}}{\mathrm{d}\tilde{\varepsilon}}\right)\frac{\eta_\mathrm{cv}}{\hbar\omega} I, \qquad (2)$$

where $\gamma_{z'x'}^{(\mathrm{e1})}$ and $\gamma_{z'x'}^{(\mathrm{hh1})}$ are constants determining the linear-in-$\mathbf{k}$ splitting of the subbands e1 and hh1; m_e and m_h are the effective masses of electrons and holes for motion in the plane of the quantum well, respectively; τ_e is the relaxation time of the spin current, which coincides with the time of relaxation

S A Tarasenko Ioffe Physical-Technical Institute,
Russian Academy of Sciences, St. Petersburg, Russian Federation
E-mail: tarasenko@coherent.ioffe.ru

Uspekhi Fizicheskikh Nauk **180** (7) 773–777 (2010)
DOI: 10.3367/UFNr.0180.201007i.0773
Translated by S N Gorin; edited by A Radzig

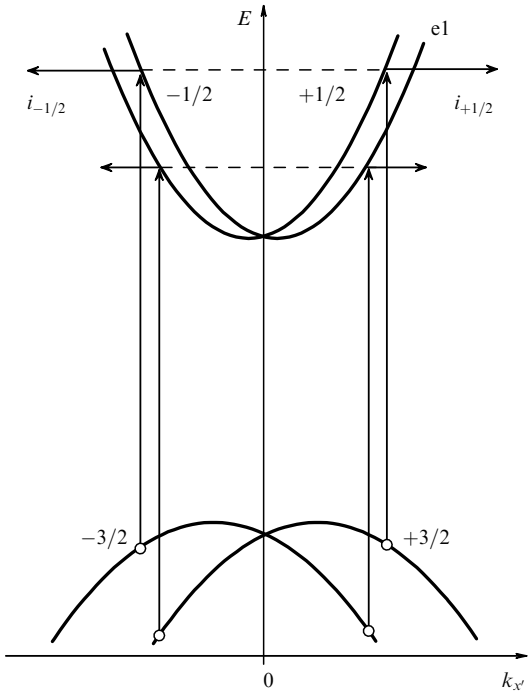

Figure 1. Mechanism of the generation of a spin current during interband optical transitions in quantum wells due to the subband splitting linear in the wave vector.

of the electron momentum if the interparticle interaction is insignificant; $\tilde{\varepsilon} = (\hbar\omega - E_g^{QW})m_h/(m_e + m_h)$ is the kinetic energy of electrons at the moment of generation; ω is the light frequency; E_g^{QW} is the effective band gap in the quantum well, and η_{cv} is the absorbed fraction of the light flux. The magnitude of the spin current (2) is determined by both the time τ_e and the derivative $d\tau_e/d\tilde{\varepsilon}$; therefore, at low temperatures the current increases significantly if the electron energy $\tilde{\varepsilon}$ is close to the energy $\hbar\Omega_{LO}$ of the optical photon. In the region of such a resonance, the spin current density can reach

$$J_{x'}^{z'} = -\frac{\tau_e^* \sqrt{2m_e\hbar\Omega_{LO}}}{2\pi} \frac{\eta_{cv}}{\hbar\omega} I, \qquad (3)$$

where τ_e^* is the time of momentum relaxation of electrons with an energy $\tilde{\varepsilon} < \hbar\Omega_{LO}$, and the time of momentum relaxation of carriers with an energy $\tilde{\varepsilon} > \hbar\Omega_{LO}$ is assumed to be much shorter.

The spin current (2) emerging during interband optical transitions near the absorption edge in the geometry of the normal light incidence is independent of the radiation polarization. The polarization dependence of spin photocurrents caused by the splitting of the spectrum arises, if we take into account the intermixing of light and heavy holes at a nonzero wave vector in the plane of the quantum well [11–13].

Another mechanism of generation of spin photocurrents is connected with the linear-in-wave-vector spin-dependent terms in the probabilities of optical transitions. Such terms appear if taking into account the **kp** admixture of states of the higher conduction band Γ_{15}^c to the wave functions of the valence band and conduction band in cubic noncentrosymmetric crystals [14]. Calculations [10] show that this contribution to the components of the spin current flowing in quantum wells with an (110) orientation during optical transitions from the subband of heavy holes is determined by the expressions

$$J_{x'}^{z'} = \beta(e_{y'}^2 - e_{x'}^2) \frac{\tau_e \tilde{\varepsilon}}{\hbar} \frac{\eta_{cv}}{\hbar\omega} I, \quad J_{y'}^{z'} = \beta e_{x'} e_{y'} \frac{\tau_e \tilde{\varepsilon}}{\hbar} \frac{\eta_{cv}}{\hbar\omega} I, \qquad (4)$$

where β is the coefficient with a dimensionality of length, which is determined by the band parameters of the semiconductor. In contrast to contribution (2), the spin photocurrent (4) strongly depends on the polarization of the exciting radiation even near the absorption edge and it does not appear during excitation by unpolarized light, when $e_{x'}^2 = e_{y'}^2 = 1/2$, and $\overline{e_{x'}e_{y'}} = 0$. A comparison of the contributions (2) and (4) shows that, depending on the light frequency, these contributions can be comparable, although one can dominate over the other.

The spatial separation of electrons with opposite spins, caused by pure spin photocurrent, was observed at room temperature in structures with GaAs/AlGaAs quantum wells in Ref. [15]. The authors used the pump–probe technique with a high spatial resolution. The linearly polarized, focused pumping pulse induced interband optical transitions; the spatial distribution of spin polarization was studied by the spin Kerr effect method using a probing light pulse with a photon energy corresponding to the band gap.

The mechanisms responsible for the generation of pure spin currents upon absorption of linearly polarized light can lead to the generation of a stationary electric current during the excitation by circularly polarized radiation. Such a circular photogalvanic effect [16] caused by interband optical transitions in quantum wells has been studied both theoretically and experimentally in Refs [17–21].

3. Intrasubband optical transitions

The main contribution to the spin current arising upon the absorption of light by free charge carriers is due to the spin-dependent asymmetry of the electron scattering processes accompanying intrasubband optical transitions. The matrix elements of electron scattering on static defects or phonons in quantum wells contain spin-dependent contributions that are odd in the wave vector [22, 23] and can be written out as

$$V_{\mathbf{k}'\mathbf{k}} = V_0 + \sum_{\alpha\beta} V_{\alpha\beta}\, \sigma_\alpha (k_\beta + k'_\beta), \qquad (5)$$

where $\mathbf{k}$ and $\mathbf{k}'$ are the initial and final electron wave vectors. Because of the asymmetry of scattering, the electrons with opposite spins, excited by light from the bottom of the size-quantized subband, pass into final states predominantly with opposite wave vectors, which does lead to the generation of pure spin current [24]. The polarization dependences of the components of the spin photocurrent have the form

$$J_x^\alpha = -\frac{\tau_e}{\hbar} \left(\frac{\langle V_0 V_{\alpha x}\rangle}{V_0^2} \frac{e_x^2 - e_y^2}{2} + \frac{\langle V_0 V_{\alpha y}\rangle}{V_0^2} e_x e_y \right) I\eta_{e1}, \qquad (6)$$

where η_{e1} is the fraction of the electromagnetic radiation that is absorbed in the quantum well upon intrasubband optical transitions and normal incidence of light, and x and y are the coordinates in the plane of the interfaces; the angle brackets stand for averaging over the scatterers. The other components of the spin photocurrent J_y^α can be obtained from formula (6) by the substitution $x \leftrightarrow y$.

The spin-dependent scattering of electrons gives rise to the generation of pure spin current not only when there is intrasubband absorption of light, but also if the electron gas is disturbed from the thermodynamic equilibrium with the crystal lattice [10]. In this situation, the spin current arises as a result of an energy relaxation of electrons on phonons, irrespective of the way in which the thermodynamic equilibrium between the electron and phonon subsystems was disturbed.

The mechanisms responsible for the appearance of spin currents with the absorption of light by free charge carriers lead to the generation of electric current if the carriers are spin-polarized, for instance, by an external magnetic field [24]. Indeed, in the case of intrasubband optical transitions, the fluxes $\mathbf{i}_{+1/2}$ and $\mathbf{i}_{-1/2}$ depend on the concentration of carriers in spin subbands, $n_{+1/2}$ and $n_{-1/2}$, respectively. In the system of spin-polarized particles in which $n_{+1/2} \neq n_{-1/2}$, the fluxes $\mathbf{i}_{+1/2}$ and $\mathbf{i}_{-1/2}$ do not compensate for each other, thus leading to the appearance of a resultant electric current. In the case of small spin polarization of electrons, the photocurrent caused by the disbalance of the spin current in the magnetic field is determined by the expression

$$j_\beta^{(\mathrm{Pol})} = 4eN_\mathrm{e} \sum_\alpha s_\alpha \frac{\partial J_\beta^\alpha}{\partial N_\mathrm{e}}\,, \tag{7}$$

where $\mathbf{s}$ is the equilibrium electron spin. The spin current J_β^α in Eqn (7) is considered formally to be a function of the concentration N_e of carriers. In particular, for a nondegenerate electron gas, when $J_\beta^\alpha \propto N_\mathrm{e}$ and $N_\mathrm{e}\partial J_\beta^\alpha/\partial N_\mathrm{e} = J_\beta^\alpha$, the photocurrent is directly proportional to the spin current.

The electric current caused by the disbalance of the spin photocurrent is most vividly manifested in structures with magnetic impurities, in which the Zeeman splitting of electronic states increases significantly due to the exchange interaction between the spins of free electrons and magnetic moments of impurities [25]. Such experiments on the detection and investigation of magnetically induced photocurrents were performed on (001)-oriented quantum wells in n-type $Cd_{1-x}Mn_xTe$ with different concentrations of manganese atoms. The photocurrent was excited by linearly polarized terahertz radiation, which caused intrasubband optical transitions, in a magnetic field oriented in the plane of interfaces. The dependences of the photo-emf on the magnetic field induction for the $Cd_{1-x}Mn_xTe$ quantum well with $x = 0.015$, obtained at various temperatures, are given in Fig. 2. It is seen that at a low temperature, $T = 1.9$ K, the photocurrent increases linearly with an increase in the magnetic field in weak fields, and saturates in fields $B \approx 6$ T. With increasing temperature, the photocurrent decreases and even changes sign, and the nonlinearity in the magnetic field disappears. Such a behavior is related to the orientation of Mn ions by the external magnetic field and qualitatively corresponds to the dependence of the Zeeman splitting of electronic states on the magnetic field and temperature in dilute magnetic semiconductors $Cd_{1-x}Mn_xTe$.

When considering the microscopic mechanisms for the generation of an electric current in structures with magnetic impurities, it is necessary to take into account that the orientation of the Mn magnetic moments by the external field results in both giant Zeeman splitting of electronic states and spin-dependent exchange scattering of free electrons by

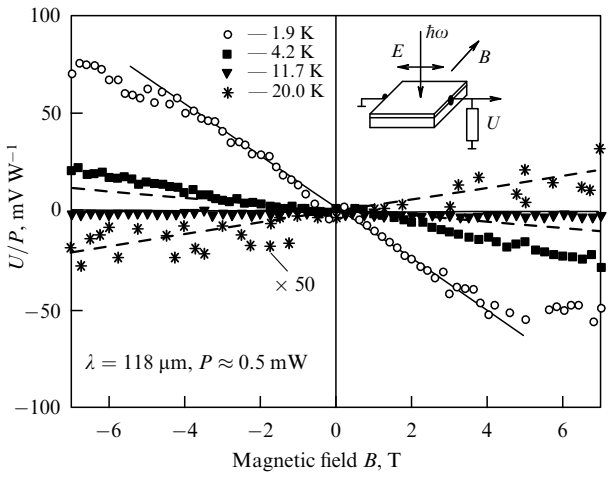

Figure 2. Dependence of the photo-emf on the magnetic field induction in a structure with a single n-type $Cd_{1-x}Mn_xTe$ quantum well upon intrasubband excitation by linearly polarized light at various temperatures. The inset to the figure shows the geometry of the experiment.

magnetic impurities. The latter effect gives rise to an additional contribution to the electric current, which is due to the difference in the momentum relaxation times of carriers in spin subbands. Indeed, in a structure with polarized Mn ions the scattering probabilities of electrons with spins oriented parallel to and against the Mn magnetic moments are different. This leads to a difference in the momentum relaxation times $\tau_{\mathrm{e},+1/2}$ and $\tau_{\mathrm{e},-1/2}$ in the spin subbands and, consequently, causes an electric current. To estimate this contribution to the photocurrent, we assume that the momentum relaxation of electrons is connected with their scattering by manganese ions, and the Hamiltonian of this interaction has the form

$$H_{\mathrm{el-Mn}} = \sum_i \left[u - \alpha(\mathbf{J}_i^{(\mathrm{Mn})}\boldsymbol{\sigma})\right] \delta(\mathbf{r} - \mathbf{R}_i)\,, \tag{8}$$

where i is the index of the impurity, $\mathbf{J}_i^{(\mathrm{Mn})}$ is the vector composed of the matrices of the total angular momentum 5/2, and $\mathbf{R}_i$ is the position of the impurity. The calculations show that the density of the electric current arising as a result of the difference in the times $\tau_{\mathrm{e},+1/2}$ and $\tau_{\mathrm{e},-1/2}$ for $|\alpha| \ll |u|$ takes on the form

$$j_\beta^{(\mathrm{Sc})} = 4e\tau_\mathrm{e} \frac{\alpha}{u} \sum_\alpha S_\alpha^{(\mathrm{Mn})} \frac{\partial J_\beta^\alpha}{\partial \tau_\mathrm{e}}\,, \tag{9}$$

where $\mathbf{S}^{(\mathrm{Mn})}$ is the average spin of Mn atoms, and J_β^α is the spin current density, which is formally considered in expression (9) as a function of τ_e. In structures with magnetic impurities, the photocurrents (7) and (9) are added.

Acknowledgments. I am grateful to E L Ivchenko, V V Bel'kov, and S D Ganichev for the fruitful discussions. This work was supported in part by the Russian Foundation for Basic Research, by a grant from the President of the Russian Federation for young scientists (MD-1717.2009.2), and by the Dinasty Foundation (CFPM).

References

1. D'yakonov M I, Perel' V I *Pis'ma Zh. Eksp. Teor. Fiz.* **13** 657 (1971) [*JETP Lett.* **13** 467 (1971)]
2. Hirsch J E *Phys. Rev. Lett.* **83** 1834 (1999)
3. Kato Y K et al. *Science* **306** 1910 (2004)
4. Wunderlich J et al. *Phys. Rev. Lett.* **94** 047204 (2005)
5. Zakharova A, Vasko F T, Ryzhii V *J. Phys. Condens. Matter* **6** 7537 (1994)
6. Perel' V I et al. *Phys. Rev. B* **67** 201304(R) (2003)
7. Bhat R D R et al. *Phys. Rev. Lett.* **94** 096603 (2005)
8. Tarasenko S A , Ivchenko E I *Pis'ma Zh. Eksp. Teor. Fiz.* **81** 292 (2005) [*JETP Lett.* **81** 231 (2005)]
9. Meier F, Zakharchenya B P (Eds) *Optical Orientation* (Amsterdam: North-Holland, 1984) [Translated into Russian (Leningrad: Nauka, 1989)]
10. Ivchenko E L, Tarasenko S A *Semicond. Sci. Technol.* **23** 114007 (2008)
11. Zhou B, Shen S-Q *Phys. Rev. B* **75** 045339 (2007)
12. Hu K G *Solid State Commun.* **148** 283 (2008)
13. Tarasenko S A *Phys. Rev. B* **72** 113302 (2005)
14. Lyanda-Geller Yu B, Pikus G E *Fiz. Tverd. Tela* **31** (12) 77 (1989) [*Sov. Phys. Solid State* **31** 2068 (1989)]
15. Zhao H et al. *Phys. Rev. B* **72** 201302(R) (2005)
16. Ivchenko E L *Usp. Fiz. Nauk* **172** 1461 (2002) [*Phys. Usp.* **45** 1299 (2002)]
17. Golub L E *Phys. Rev. B* **67** 235320 (2003)
18. Khurgin J B *Phys. Rev. B* **73** 033317 (2006)
19. Bel'kov V V et al. *Solid State Commun.* **128** 283 (2003)
20. Bieler M et al. *Appl. Phys. Lett.* **86** 061102 (2005)
21. Yang C L et al. *Phys. Rev. Lett.* **96** 186605 (2006)
22. Averkiev N S, Golub L E, Willander M *J. Phys. Condens. Matter* **14** R271 (2002)
23. Ivchenko E L, Tarasenko S A *Zh. Eksp. Teor. Fiz.* **126** 426 (2004) [*JETP* **99** 379 (2004)]
24. Ganichev S D et al. *Nature Phys.* **2** 609 (2006)
25. Ganichev S D et al. *Phys. Rev. Lett.* **102** 156602 (2009)

PACS numbers: **75.76.+j**, **76.30.–v**, **85.75.–d**
DOI: 10.3367/UFNe.0180.201007j.0777

Spin relaxation anisotropy in two-dimensional semiconductors

N S Averkiev

1. Introduction

The main task of the new field in electronics — spintronics — is the creation of devices which use spin degrees of freedom for the storage, recording, and readout of information. Contemporary electronics is oriented toward the use of two-dimensional semiconductor structures with a high mobility of charge carriers; therefore, a fundamental problem of studying the processes of spin dynamics precisely in low-dimensional nanostructures exists. The main difference between two-dimensional structures and bulk semiconductors is the anisotropy of physical properties caused by the restriction of the motion of charge carriers along one crystallographic direction. The main properties of spin dynamics are also connected with this very feature, although the spin can be oriented in any of the three spatial directions, even in two-dimensional systems. Spin relaxation constitutes a process of the disappearance of the ensemble-averaged spin of charge carriers. Indeed, spin–orbit interaction in each microscopic scattering event can result in a change of the sign of the electron-spin projection onto a preferred axis to the opposite sign. The total magnitude of the square of the spin momentum remains unaltered in this case. The process of the loss of the average spin upon the interaction of electrons with, for example, impurities can be described in terms of the following kinetic equations

$$\dot{n}_\uparrow = -Wn_\uparrow + Wn_\downarrow\,, \quad \dot{n}_\downarrow = -Wn_\downarrow + Wn_\uparrow, \tag{1}$$

where $n_\uparrow$ and $n_\downarrow$ are the numbers of electrons with spins up and down, respectively, and W describes the rate of transitions with spin flips. It follows from Eqn (1) that $\dot{n}_\uparrow + \dot{n}_\downarrow = 0$, and for the total spin $S = (n_\uparrow - n_\downarrow)/2$ we obtain

$$\dot{S} = -\frac{S}{\tau_s}\,, \quad \tau_s^{-1} = 2W, \tag{2}$$

where τ_s is the spin relaxation time. Equation (2) describes the disappearance of the average spin because of the spin flip in each scattering event. The quantity W can be due to the spin–orbit interaction (Elliott–Yafet mechanism of spin relaxation) or by the contact magnetic interaction of an electron or a hole with magnetic ions. However, in semiconductors at not too low temperatures the most significant mechanism of spin relaxation is the kinetic mechanism suggested by D'yakonov and Perel' [1]. In terms of this mechanism, the disappearance of the average spin occurs not at the instant of scattering, but rather between the instants of collisions, because of the precession of an electron spin in the effective magnetic field caused by spin–orbit interaction. Indeed, in a magnetic field the spin precesses about the field vector in such a manner that only the spin projection onto the field direction is retained, while the average values of the transverse components of the spin are lost. However, if this effective field changes direction, the relaxation of all spin components will occur. This process can be described by the following equation

$$\dot{\mathbf{S}} + \mathbf{S}\times\boldsymbol{\Omega} = \frac{\langle\mathbf{S}\rangle - \mathbf{S}}{\tau}\,, \tag{3}$$

where $\boldsymbol{\Omega}(\mathbf{k})$ is the frequency of spin precession in the effective magnetic field; $\mathbf{S}(\mathbf{k})$ is the spin density of the ensemble of electrons; $\langle\mathbf{S}\rangle$ is the value of $\mathbf{S}$ averaged over the angles of the vector $\mathbf{k}$, and τ is the time of isotropization of the electron distribution function over the angles of the vector $\mathbf{k}$. When deriving Eqn (3), it was assumed that the time of energy relaxation is much greater than τ and, thus, $\mathbf{S}(\mathbf{k})$ represents the spin density at a fixed energy. In addition, it was assumed that in formula (3) the electron lifetime is much greater than the spin relaxation time τ_s. Usually, the time τ proves to be on the order of the time of the momentum relaxation, and $\Omega\tau \ll 1$ (with $\langle\boldsymbol{\Omega}\rangle \equiv 0$). In this case, the angle of rotation between collisions proves to be small, so that the spin relaxation will occur via particle diffusion. As is seen from Eqn (3), the components of $\mathbf{S}$ that are dependent on the angles of the vector $\mathbf{k}$ relax in a time τ, and the average spin relaxes in a longer time and, in view of the inequality $\Omega\tau \ll 1$, the time of spin relaxation should be relatively large, $\tau_s \gg \tau$. It can be

N S Averkiev Ioffe Physical-Technical Institute,
Russian Academy of Sciences, St. Petersburg, Russian Federation
E-mail: averkiev@les.ioffe.ru

Uspekhi Fizicheskikh Nauk **180** (7) 777 – 780 (2010)
DOI: 10.3367/UFNr.0180.201007j.0777
Translated by S N Gorin; edited by A Radzig

shown that the equation for the average spin $\langle S\rangle$ takes on the form [1, 2]

$$\langle \dot{S}_i\rangle = -\tau\Big[\langle \mathbf{\Omega}^2\rangle\langle S_i\rangle - \sum_j \langle \Omega_i\Omega_j\rangle\langle S_j\rangle\Big]. \qquad (4)$$

Equation (4) was derived on the assumption that τ is independent of energy, and from this follows that $\tau_s^{-1} \sim \Omega^2\tau$, i.e., the relaxation becomes more efficient with increasing τ. This means that in samples with a high mobility, where τ is large, the spin relaxation can be efficient even at a weak spin–orbit interaction.

It will be shown in Sections 2–4 how spin relaxation occurs in two-dimensional semiconductor structures in terms of the D'yakonov–Perel' kinetic mechanism.

2. Anisotropy of spin relaxation in asymmetric quantum wells

In two-dimensional structures, the dependence of the precession frequency $\mathbf{\Omega}(\mathbf{k})$ is determined by two factors. First, because of the asymmetry of the well itself, the Rashba effect occurs [3], which leads to the following $\mathbf{\Omega}(\mathbf{k})$ dependence:

$$\mathbf{\Omega} = \alpha(k_y, -k_x)\,, \qquad (5)$$

where α is a coefficient. Second, for semiconductor structures grown on the basis of semiconducting III–V compounds, even in symmetrical wells grown along the (001) axis, there arises a contribution to $\mathbf{\Omega}(\mathbf{k})$ which is called the Dresselhaus contribution [2, 4]:

$$\mathbf{\Omega} = \beta(k_x, -k_y)\,, \qquad (6)$$

where β is a parameter differing from α. The substitution of expressions (5) and (6) into equation (4) makes it possible to obtain the spin relaxation times. For asymmetrical quantum wells grown along the (001) axis, the calculations of the relaxation times for the spin orientation along the (001) axis (τ_z), (1$\bar{1}$0) axis (τ_+), and (110) axis (τ_-) yield

$$\tau_z^{-1} = C(\alpha^2+\beta^2)\,, \quad \tau_+^{-1} = \frac{1}{2}\,C(\alpha+\beta)^2\,,$$
$$\tau_-^{-1} = \frac{1}{2}\,C(\alpha-\beta)^2\,, \quad C = \tau k^2\,. \qquad (7)$$

An important circumstance is that the parameter α is determined by the shape of the quantum well and can change upon application of an electric field. In addition, it is seen from formulas (7) that at $\alpha = \pm\beta$ one of the times can become infinitely large, which means the absence of spin relaxation for spins oriented in the plane of the quantum well along the direction (110) or (1$\bar{1}$0). The possibility of such an anisotropy was noted in Ref. [5], and was observed for the first time in Ref. [6] in the dependence of the Hanle effect on the orientation of the magnetic field in the quantum-well plane. The effect has been demonstrated most vividly in Ref. [7], where the spin relaxation of electrons was investigated in double quantum wells in which the ratio α/β was controlled using an external electric field (Fig. 1). It is seen from Fig. 1 that, at $V \approx 1.2$ V and $\alpha = 0$, the times τ_+ and τ_- coincide, while at $V \approx 0.7$ V and $\alpha = \beta$, they differ severalfold. In addition, it follows from the results shown in Fig. 1 that the lifetime τ_0 exceeds the spin relaxation times τ_+ and τ_- severalfold; therefore, the total time T_s of the spin

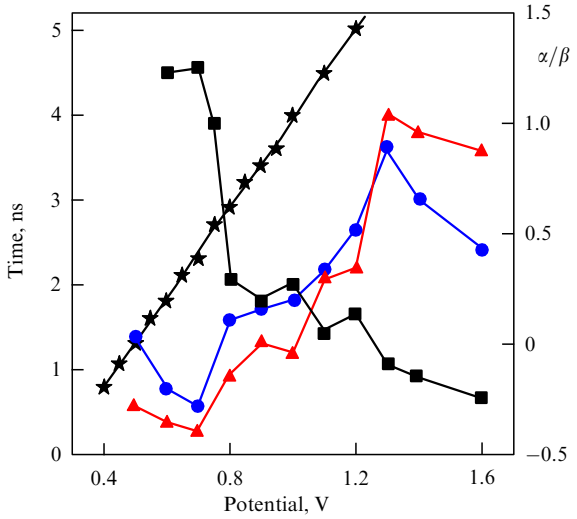

Figure 1. Anisotropy of spin relaxation in the plane of a quantum well depending on an external electric field: ▲ — τ_+, ● — τ_-, ■ — α/β, and (★) — radiative lifetime τ_0 of electrons.

disappearance, which is equal to $\tau_0\tau_s/(\tau_0+\tau_s)$, virtually coincides with τ_s.

Another (more obvious) anisotropic effect is the dependence of the relaxation time on the spin orientation relative to the growth axis: the relaxation rate of spin oriented along the growth axis is twice as large as the relaxation rate of spin lying in the plane of the quantum well. The reason for this effect is that if the spin is oriented along the growth axis (z), it is subject, according to expressions (5) and (6), to the effective field directed along the x- and y-axes. If the spin lies in the plane of the well (e.g., along the x-axis), its relaxation is affected only by the effective magnetic field directed along the y-axis. This leads to an increase in the spin relaxation times τ_+ and τ_-. Notice that an exactly twofold difference in the relaxation times is realized only if $\alpha = 0$ or $\beta = 0$.

The anisotropy of the relaxation rate in two-dimensional systems also arises in the case of the Elliott–Yafet mechanism of spin relaxation. It can be shown that in two-dimensional structures the spin-dependent electron scattering is described by the expression [8]

$$V'_{kk'} = V_0(\mathbf{k}-\mathbf{k}')\big[\boldsymbol{\sigma}\times(\mathbf{k}+\mathbf{k}')\big]_z\,, \qquad (8)$$

where $\mathbf{k}$ and $\mathbf{k}'$ are the initial and final quasimomenta of the electron in the plane of the quantum well; z is the growth axis; $V_0(\mathbf{k}-\mathbf{k}')$ is the Fourier image of the scattering potential; $\boldsymbol{\sigma} = (\sigma_x, \sigma_y, \sigma_z)$, and σ_i are the Pauli matrices. A specific feature of Eqn (8) is a linear dependence of V' only on the transverse components of the vectors, k_x and k_y or k'_x and k'_y. As a result, the effective field leading to the relaxation of spin oriented along the z-axis can be oriented along the x- and y-axes, whereas in the case of spin that is parallel to the x-axis, only along the y-axis. It is this feature that leads to a twofold difference in the appropriate times. A calculation with allowance for the 'golden rule' yields the expressions [8]

$$\frac{1}{\tau_{zz}} = \frac{2}{\tau_{xx}} = \frac{2}{\tau_{yy}}\,, \qquad \frac{1}{\tau_{zz}} = \frac{1}{\tau_p}\,\frac{\Delta}{E_g}\,\frac{k_B T}{E_g}\,, \qquad (9)$$

where Δ is the magnitude of spin–orbit splitting in the valence band; E_g is the forbidden band width; τ_p is the momentum

relaxation time, which is inversely proportional to $|V_0|^2$; T is the temperature, and k_B is the Boltzmann constant. In a bulk cubic crystal, all the times are equal and proportional to $(k_B T/E_g)^2$.

3. Spin relaxation in degenerate semiconductor structures

As follows from formulas (7), the spin relaxation time τ_s in terms of the kinetic mechanism is inversely proportional to the time τ of isotropization of the distribution function, which, in turn, is proportional to the momentum relaxation time. This means that in heavily doped bulk crystals the kinetic mechanism will be suppressed because of the small momentum-relaxation time τ_p. In two-dimensional systems, the impurities can be spatially separated from the electrons; then, in heavily doped structures τ_p also proves to be large, so that we obtain $\Omega\tau_p \sim 1$. In this case, the problem of the role of electron–electron collisions in the process of spin relaxation arises. A specific feature of the situation is also that electron–electron interactions do not affect the momentum relaxation time, since in such interactions the total momentum of the system remains unaltered.

It was first shown in Ref. [9] that if in the collision integral in equation (2) for $\mathbf{S}(\mathbf{k})$ we take into account only electron–electron collisions, then the spin relaxation in the regime of the D'yakonov–Perel' mechanism takes place. The microscopic reason for the relaxation, as before, is the spin precession in the effective magnetic field $\mathbf{\Omega}(\mathbf{k})$, and the interaction of particles leads to the isotropization of the distribution function, so that the time τ of the isotropization of the distribution function proves to be equal to $\tau_p\tau_{ee}/(\tau_p + \tau_{ee})$, where τ_{ee} is the isotropization time due to electron–electron collisions.

An important feature of the D'yakonov–Perel' mechanism during frequent electron–electron interactions is a sharp temperature dependence of τ_s caused by the fact that in a degenerate electron gas the isotropization time of the distribution function may be estimated as $\tau \sim 1/T^2$. Combined experimental and theoretical investigations (see Fig. 2) have shown that such a relaxation of spins does take place. At high temperatures, $T \sim T_F$, the results of calculations with allowance for electron–electron collisions demonstrate good agreement with experimental data. The theoretical curve (dashed line) was constructed using formulas analogous to Eqn (7) at $\beta = 0$ under the condition that the time τ_p is estimated from the temperature dependence of mobility. At low temperatures, $T \sim 5$ K, electron–electron collisions are suppressed and the result of the calculation (dashed line) demonstrates agreement with the experimental data (open squares). It has been shown in Section 2 that the anisotropy of the processes of spin relaxation is caused by the dependence of the effective magnetic field on the electron momentum rather than by the processes of isotropization of the distribution function. This means [10] that in the case of an efficient electron–electron interaction as well, when $\mathbf{\Omega}(\mathbf{k})$ is caused simultaneously by the Rashba and Dresselhaus effects, a dependence of the rate of spin relaxation on the spin orientation in the plane of the quantum well arises.

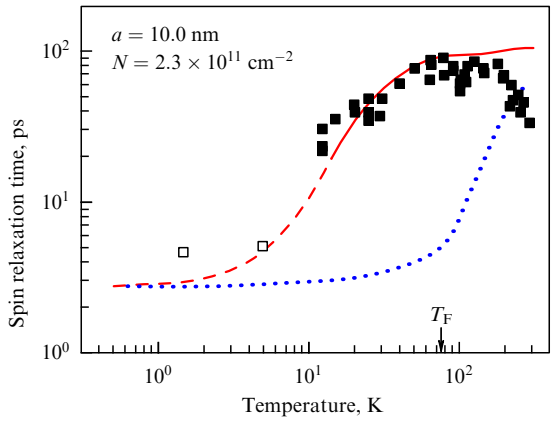

Figure 2. Temperature dependence of the spin relaxation time of an electron gas: a, the width of the quantum well; N, the concentration of electrons; T_F, the temperature of the degeneracy of the electron gas; ■, experimental data [10]; solid curve, theoretical results [10] for $\Omega\tau \ll 1$. The result of the corresponding calculation without allowance for electron–electron collisions at low temperatures, $\tau_{ee} \gg \tau_p$, is shown by a dashed line; □, experimental results [10].

4. Anisotropy of spin relaxation in structures grown along the (110) axis

As is seen from Eqn (4), in the general form the spin relaxation is described by a second-rank tensor relating the rate of changes in the average spin to the spin magnitude itself. In cubic crystals, such a tensor reduces to a scalar, but in low-symmetry two-dimensional structures the tensor of the inverse relaxation times is characterized by three independent parameters. The principal axes of the tensor of the spin-relaxation times can be noncoincident with the natural geometric axes of the sample. As was first indicated in Ref. [12], such a case is realized in asymmetrical wells grown along the (110) axis. In structures with such a crystal orientation, the relaxation of spin oriented at the initial instant of time along the growth axis will lead to the appearance of a spin component oriented in the plane of the quantum well. A microscopic reason for this effect in structures with the growth axis (110) may be the combined action of the Rashba and Dresselhaus effects. Indeed, for such structures the effective magnetic field caused by the Dresselhaus effect has only a z-component, but depends on k_x (Fig. 3). The Rashba field has components B_x and B_y proportional to k_y and k_x, respectively. It is shown in Fig. 3 that one of the proper axes of the tensor of spin-relaxation times will coincide with the x-axis, and two other axes will make angles θ with the y- and z-axes. The results of the calculations [12] (see Fig. 3) demonstrate that at $\alpha \sim \beta$ and times of the order of τ_s the spin component S_y can reach $\sim 10\%$ of the initial value S_{z0}.

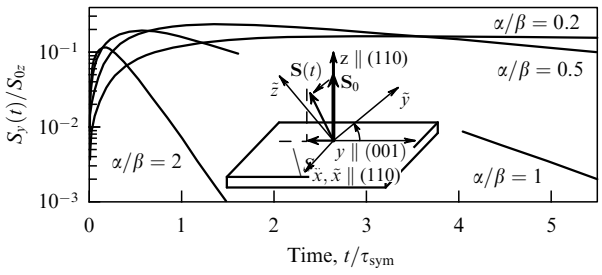

Figure 3. Generation of spin density S_y in asymmetrical quantum wells because of the anisotropy of spin relaxation: S_{0z}, the magnitude of the initial spin orientation along the z-axis, and τ_{sym}, the spin relaxation time in a symmetrical quantum well.

5. Conclusions

In this paper, we considered the main features of the anisotropy of spin relaxation for electrons in low-dimensional semiconductors. It has been shown that the anisotropy arises both because of natural causes (the presence of a growth axis, and the restriction of the free motion in this direction) and as a result of the mutual action of the Rashba and Dresselhaus effects. It is basical that the magnitude of α can be controlled using technological means or an external electric field.

Because of the anisotropy of spin-relaxation times, the spin does not relax along some directions in the plane of the quantum well, which opens up the possibility of using the anisotropy effect for spin storage.

It can be shown that in quantum wells where the majority carriers are holes such effects can also show themselves, although some important features exist in this case, since the total projection of the hole momentum, $\pm 3/2$ or $\pm 1/2$, is always oriented along the growth axis.

Acknowledgments. I am grateful to M M Glazov, L E Golub, and S A Tarasenko for the fruitful discussions, and to N I Sablina for assistance in the work. This work was supported in part by the Russian Foundation for Basic Research (project No. 08-02-00069a), and by the Federal Target Program 'Scientific and Pedagogical Personnel of Innovative Russia' (project 02.740.11.5097).

References

1. D'yakonov M I, Perel' V I *Zh. Eksp. Teor. Fiz.* **60** 1954 (1971) [*Sov. Phys. JETP* **33** 1053 (1971)]
2. D'yakonov M I, Kachorovskii V Yu *Fiz. Tekh. Poluprovodn.* **20** 178 (1986) [*Sov. Phys. Semicond.* **20** 110 (1986)]
3. Rashba E I *Fiz. Tverd. Tela* **2** 1224 (1960) [*Sov. Phys. Solid State* **2** 1109 (1960)]
4. D'yakonov M I, Perel' V I *Fiz. Tverd. Tela* **13** 3581 (1971) [*Sov. Phys. Solid State* **13** 3023 (1971)]
5. Averkiev N S, Golub L E *Phys. Rev. B* **60** 15582 (1999)
6. Averkiev N S et al. *Phys. Rev. B* **74** 033305 (2006)
7. Larionov A V, Golub L E *Phys. Rev. B* **78** 033302 (2008)
8. Averkiev N S, Golub L E, Willander M *J. Phys. Condens. Matter* **14** R271 (2002)
9. Glazov M M, Ivchenko E L *Pis'ma Zh. Eksp. Teor. Fiz.* **75** 476 (2002) [*JETP Lett.* **75** 403 (2002)]
10. Leyland W J H et al. *Phys. Rev. B* **75** 165309 (2007)
11. Glazov M M, Ivchenko E L *Zh. Eksp. Teor. Fiz.* **126** 1465 (2004) [*JETP* **99** 1279 (2004)]
12. Tarasenko S A *Phys. Rev. B* **80** 165317 (2009)